

**A STUDY OF BONDING MECHANISMS OF
CORRUGATING MEDIUM**

Project 2696-17

**Report Two
A Progress Report
to**

**FOURDRINIER KRAFT BOARD GROUP
of The
AMERICAN PAPER INSTITUTE**

November 3, 1978

THE INSTITUTE OF PAPER CHEMISTRY

Appleton, Wisconsin

A STUDY OF BONDING MECHANISMS OF CORRUGATING MEDIUM

Project 2696-17

Report Two

A Progress Report

to the

FOURDRINIER KRAFT BOARD GROUP

of the

AMERICAN PAPER INSTITUTE

Information contained herein is furnished for your internal use only and is not to be disseminated or disclosed outside your company nor copied or otherwise reproduced without the express written permission of The Institute of Paper Chemistry

November 3, 1978

TABLE OF CONTENTS

	Page
SUMMARY	
INTRODUCTION	1
Problem Review	1
Historical Background	2
Previous Work	3
Film Thickness Measurements	3
Analytical Model	5
Film Instabilities	6
RESEARCH OBJECTIVES	10
Pressure Measurements	10
Photographs of Instabilities	11
Analytical Model	11
EXPERIMENTAL APPARATUS	12
Rebuilt Applicator	12
Pressure Measurements	12
Photographs of Surface Phenomena	18
RESULTS	19
Pressure Measurements	19
Film Stability Photographs	26
ANALYTICAL MODELS	32
Film Thickness Predictions	32
Modeling Surface Phenomena	35
Free Surface Energy	38
Kinetic Energy	38
CONCLUSIONS AND SUGGESTIONS FOR FUTURE WORK	42
Pressure Measurements	42
Analytical Model for Film Thickness	42

	Page
Film Stability Photographs	43
Modeling Film Instabilities	43
Suggestions for Future Work	44
NOMENCLATURE	46
LITERATURE CITED	48
APPENDIX.	50

SUMMARY

The results of the second portion of an investigation of a reverse-roll corrugating adhesive applicator are reported and are summarized by the following:

1. Measurements were made of the fluid static pressure distributions in the nip between two rolls. The pressure distributions are used to determine the quantities needed to complete an analytical model which was described in the first progress report and predicts the film thickness on the applicator roll for various operating conditions. However, the distances within the nip could not be determined with sufficient spatial resolution to be used in the model. Nevertheless, the pressure pulses did provide information about the magnitude of the pressure under the nip and suggest that the motion of the film splitting locations in the nip coincides with the occurrence of the speed ratio that produces a uniform film thickness through a range of speeds.
2. The model for predicting the film thickness was found to be very sensitive to several parameters, all of which are difficult to quantify. As a result, the model appears to be impractical, and a simple regression analysis of the important parameters is suggested as a more practical approach to modeling the film thickness.
3. Photographs of the adhesive film thickness on the surface of the applicator roll suggest that the instabilities are not severe problems at normal operating conditions. The ringing

phenomenon occurs at low speed ratios and is more intimately connected to the operating conditions of the applicator than to the fluid properties of the adhesive. The blotches and stripping appear to be interrelated and equally dependent upon the operating conditions and fluid properties. Additionally they are affected by the roll surface conditions. These phenomena occur at considerably higher speed ratio for most adhesives.

4. Several new and important topics for future fundamental research were suggested as a result of the findings of this project. These investigations could provide useful information concerning the coating process as well as corrugating glue application.

A STUDY OF BONDING MECHANISMS OF CORRUGATING MEDIUM

INTRODUCTION

PROBLEM REVIEW

The common means of applying adhesive to the flute tips of corrugated medium is shown in Fig. 1 and is referred to as a reverse-roll applicator system. A layer of glue adheres to the surface of the applicator roll as it rotates in the adhesive tray. The adhesive is then forced into the nip area where most of it is sheared from the applicator roll. Only a thin film passes through the nip and is translated onto the surface of the applicator roll to where it contacts the flute tips of the medium. A small amount of adhesive is retained on the flute tip in preparation for bonding with the liner.

ADHESIVE APPLICATOR SYSTEM

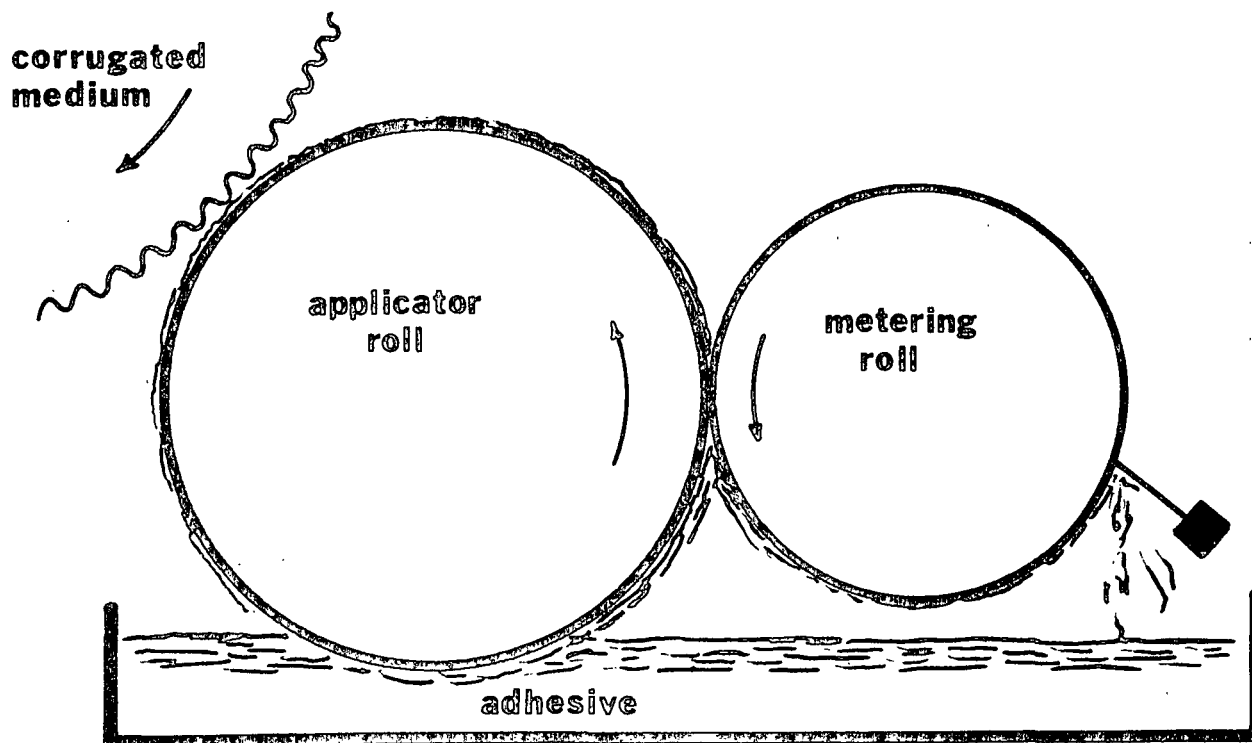


Figure 1. Reverse Roll Glue Applicator System

Controlling the thickness and uniformity of the film on the surface of the applicator roll is difficult for many reasons. Some of the difficulties are related to the mechanics of the applicator system: nonparallel rolls, roll roundness, bearings, etc. Besides these mechanical factors, the fluid dynamics of the adhesive pickup and metering are complex and poorly understood. Additionally, the film on the surface of the applicator roll after it has been metered in the nip often becomes unstable and exhibits surface patterns which could adversely affect the uniformity of applied film. The transfer of adhesive is another important problem, and little research has been devoted to describing the transfer mechanisms.

The objective of this entire project is to obtain information on all aspects of the application process and use the information to improve the performance of existing applicators.

HISTORICAL BACKGROUND

Project 2696-17 was initiated to study the adhesive bonding mechanisms of corrugated medium. In particular, the objective was to understand the process by which adhesive is transferred from the applicator roll to the flute nips of the corrugated medium. The initial work involving surface receptivity (1) and the surface roughness of the medium proved unsuccessful, and it was concluded that in order to properly examine the adhesive bonding mechanisms, the dynamics of the applicator system must be described. A new project was then designed to study the mechanics of the system and was divided into two phases. The first phase was a study of the metering of the adhesive film and the translation of the film onto the surface of the applicator roll. The second phase would examine the transfer of the adhesive from the applicator roll to

the flute tips of the medium. This is the second progress report pertaining to the first phase of the project.

PREVIOUS WORK*

The first portion of Phase I of the project dealt with describing the metering process that occurs in the nip region between the rolls. Experimental measurements of the adhesive film thickness were made at various operating conditions, and an analytical model to describe the fluid mechanics was developed.

Film Thickness Measurements

An experimental laboratory applicator was built to the dimensions of typical industrial units. A sample of fluid was scraped from the surface of the applicator roll and used to determine an average film thickness for a variety of fluids at several operating conditions. The results for a common starch adhesive showed that there was a ratio of the metering roll to applicator roll surface speed for which the film thickness on the applicator roll remained constant regardless of the corrugator speed. This speed ratio is evident when the experimental data is plotted as shown in Fig. 2. Setting the speed ratio on the applicator to this value obviously eliminates the variation in the film thickness with the speed of the applicator. When other fluids were tested, it was found that the magnitude of the crossover speed ratio was not unique. Since speed changes occur frequently on a corrugator and starch compositions are often varied, it was nearly impossible to predict the thickness of the film from knowledge of the operating conditions. However, after detailed investigation, a correlation was found between the fluid viscosity and the desired speed ratio

*For more details concerning the initial results of the project the reader is referred to Progress Report One (Ref. 2).

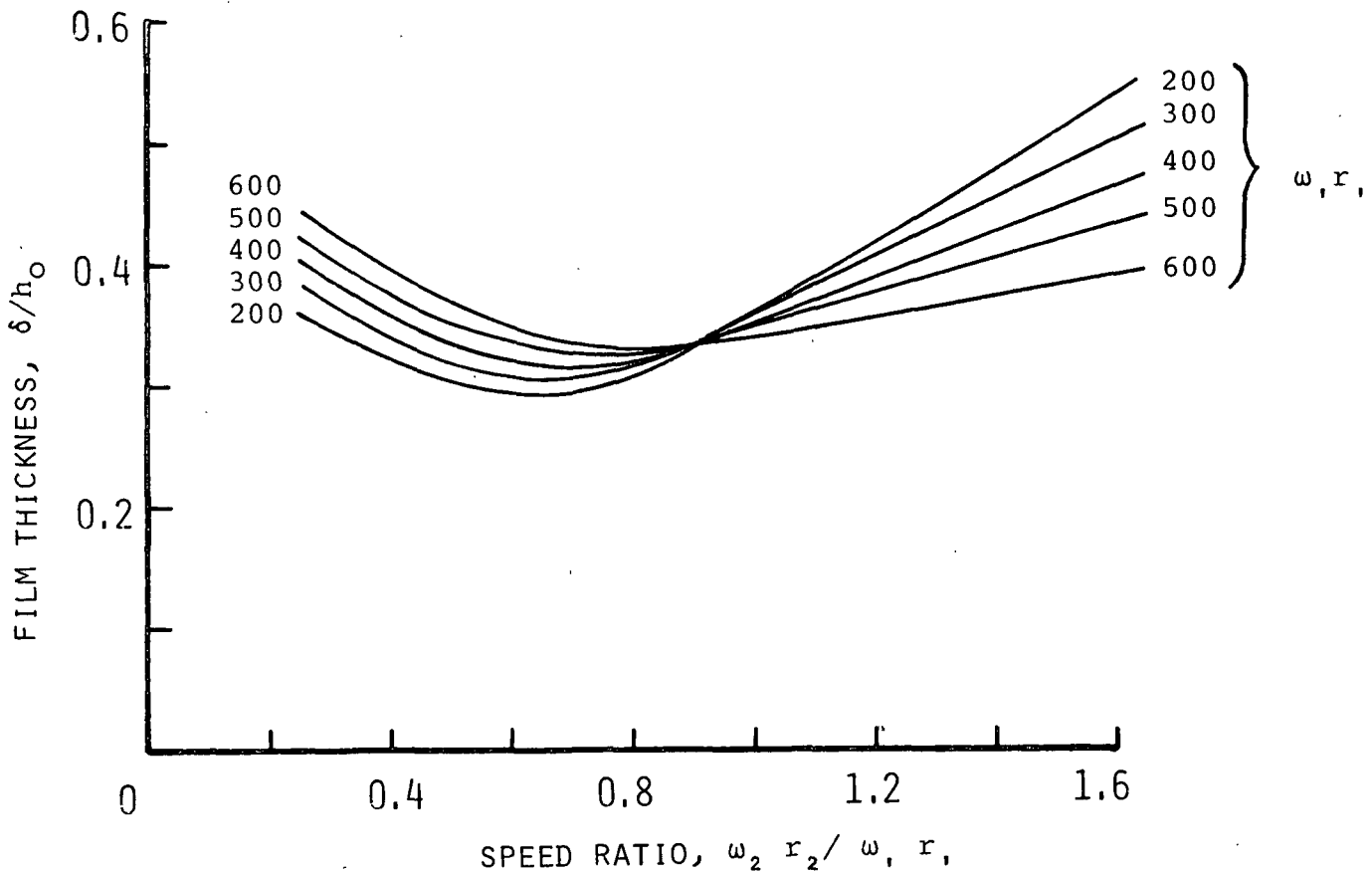


Figure 2. Effect of Speed Ratio on Surface Film Thickness

(see Fig. 3). The importance of the relationship is that the proper setting for the speed ratio could now be determined by simply knowing the fluid viscosity. Even with this information the prediction of film thicknesses is not totally resolved since the curve is very steep in the region where most adhesives lie, and viscosity measurements are not extremely accurate or well defined for starch adhesives under these conditions.

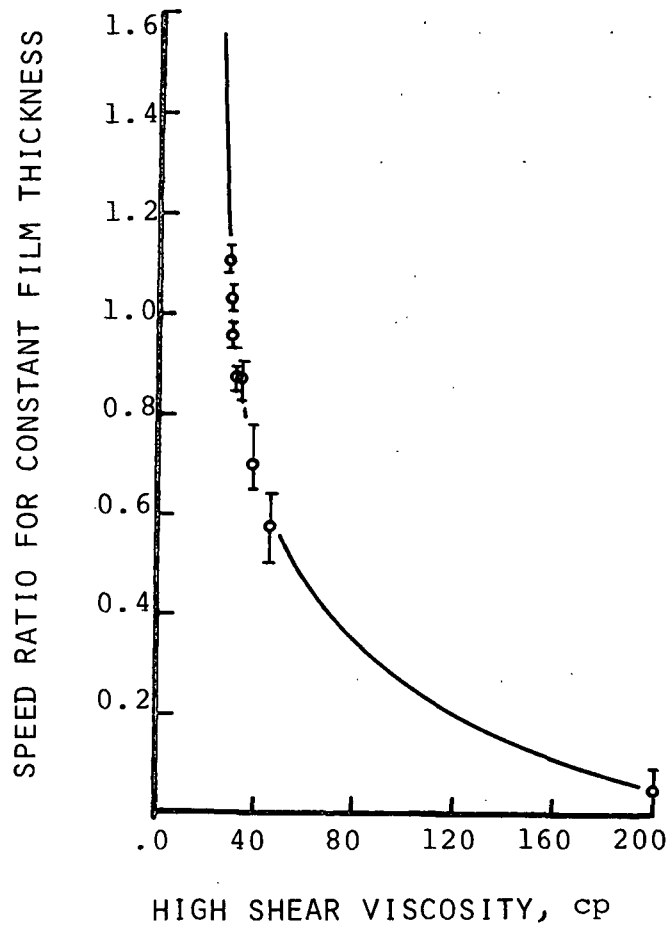


Figure 3. Effect of Viscosity on Optimum Speed Ratio

Analytical Model

An analytical model was developed to describe the flow between the two rolls and determine the ultimate film thickness on the applicator roll. The model was based upon a time-dependant Couette flow and resulted in an expression for film thickness [Equation (1)]:

$$\delta_a = (1 - u_m/u_a) h_m/2 + 4/\pi^2 (1 + u_m/u_a) h_m e^{-\pi^2 vt/h_m^2} \quad (1)$$

where δ_a = film thickness
 u_m = metering roll speed
 u_a = applicator roll speed

\underline{h}_m = gap spacing at maximum pressure location

\underline{t} = time fluid has been sheared

ν = fluid kinematic viscosity

The model was incomplete since both \underline{h}_m and \underline{t} are unknown quantities. However, if the fluid static pressure distribution in the nip could be determined experimentally, the two parameters could be estimated and the solution would be closed (see Report One). Determining the pressure distributions was one of the prime objectives of the second part of the project.

Film Instabilities

In the process of obtaining the film thickness measurements on the laboratory applicator, three different forms of surface film phenomena were observed. The first and most common was a "ring" pattern around the circumference of the roll (Fig. 4). The rings seemed to be more predominant at low speed ratios and were initially attributed to the formation of Taylor vortices in the nip. Another form of surface phenomenon was a "blotching" or "tracking" behavior of the film (Fig. 5), and the most severe surface condition from the standpoint of glue application was a complete stripping of the adhesive from the roll surface (Fig. 6). No explanation was offered for the last two phenomena.

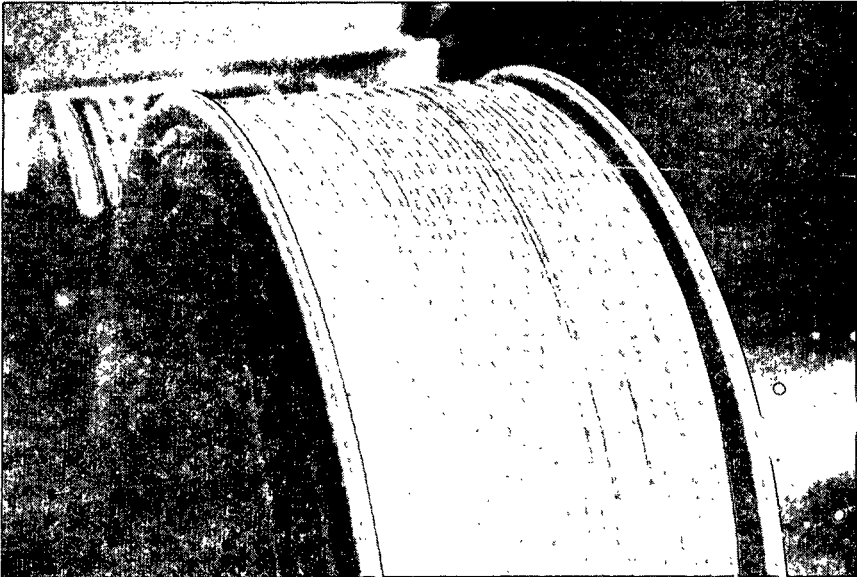
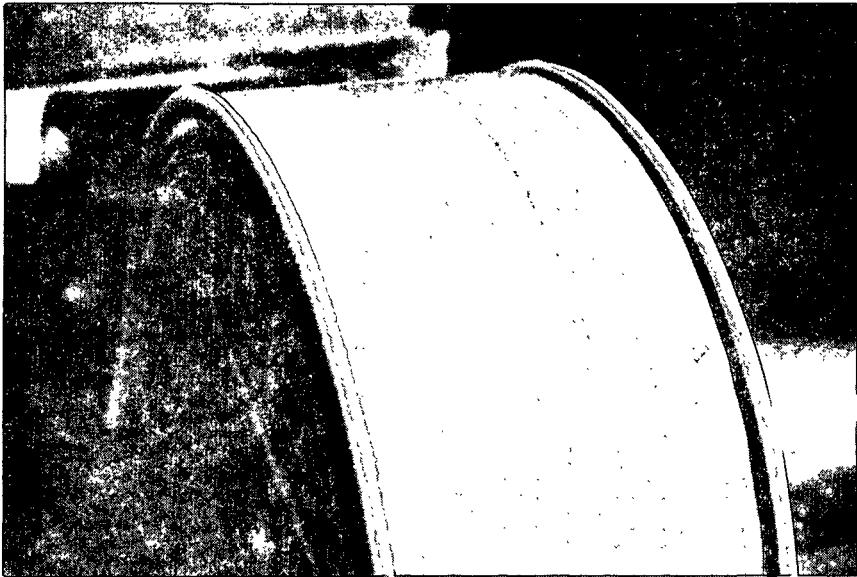


Figure 4. Ring Instability

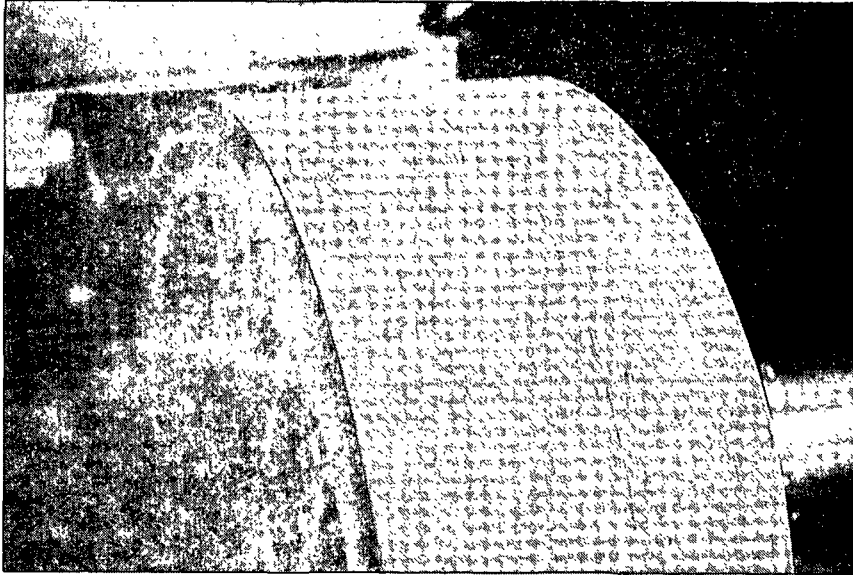


Figure 5. Surface Blotch Instability

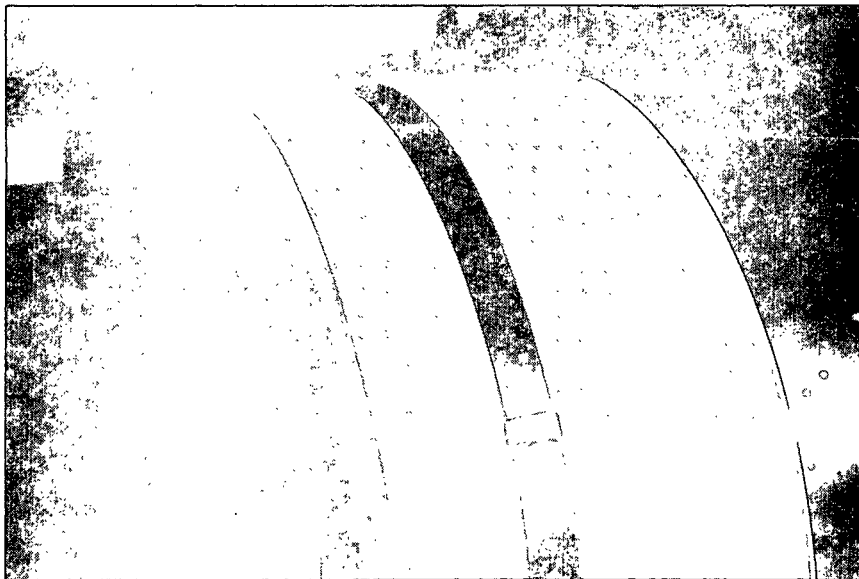


Figure 6. Roll Stripping

RESEARCH OBJECTIVES

PRESSURE MEASUREMENTS

Two parameters, \underline{h}_m , the gap spacing between the rolls, and \underline{t} , the time the fluid has been sheared, were required to complete the analytical model. It was proposed that they be determined from a fluid static pressure distribution within the nip. The distribution was to be obtained by embedding a pressure transducer in the surface of the applicator roll. A series of pressure profiles for various operating conditions would be generated in order to empirically define \underline{h}_m and \underline{t} as a function of the operating conditions. The location of the point of maximum pressure, \underline{x}_m (Fig. 7), is used to calculate the gap spacing

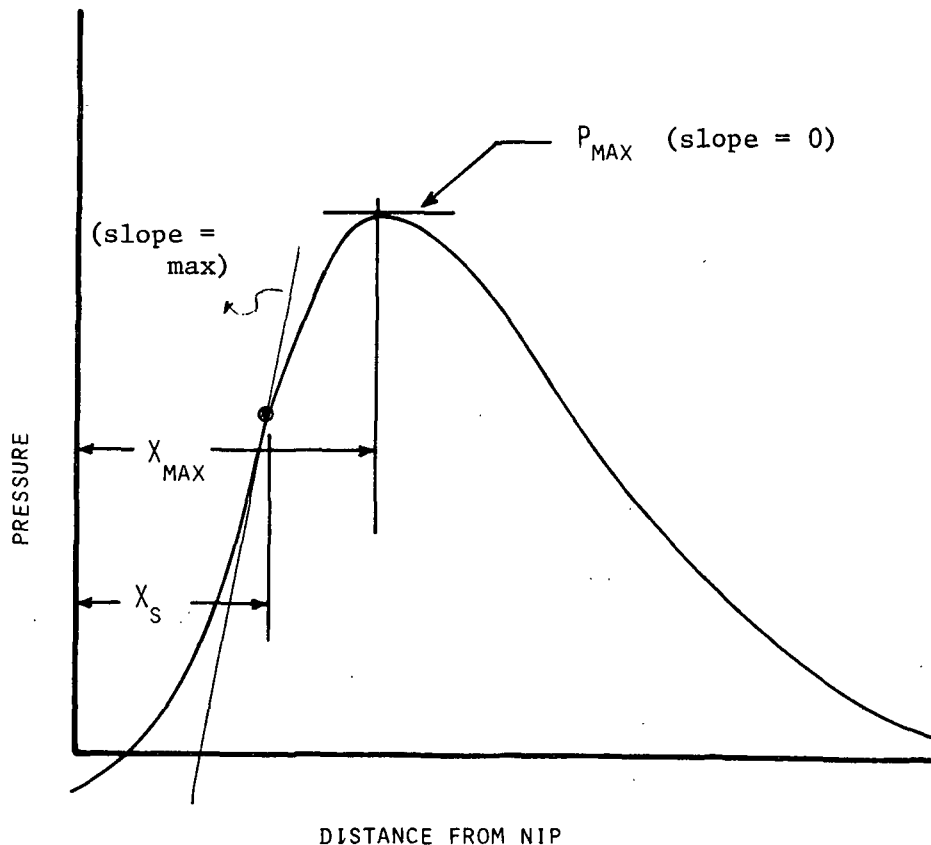


Figure 7. Pressure Distribution in the Nip

\underline{h}_m (\underline{h}_m is a quadratic function of \underline{x}_m). Similarly, if the fluid is assumed to separate from the metering roll at the point of maximum slope of the pressure distribution, then the shearing time \underline{t} can be calculated from the distance between the maximum pressure and the point of maximum pressure gradient. The distance \underline{x}_s divided by the relative surface speed ($\underline{x}_s/v_{\text{surface}} = \underline{t}_{\text{shear}}$) is the shearing time (see Report One).

PHOTOGRAPHS OF INSTABILITIES

Another objective of the project was to define the operating conditions at which the film instabilities occur. This would provide the operator of a corrugator with information concerning what conditions should be avoided. Also, the detailed mapping of operating conditions will provide some insight about the origins of the instabilities.

ANALYTICAL MODEL

There were two objectives relating to the analytical model. The first was to evaluate the model for predicting film thickness presented in Report One using the experimental pressure measurements to complete the model. The second was to develop an analytical model that would define and predict the surface instabilities observed on the applicator roll.

EXPERIMENTAL APPARATUS

REBUILT APPLICATOR

In order to complete the new objectives of the project, the experimental applicator was redesigned. In the original configuration, the shafts were supported at the side plates (see Fig. 8). The metering roll was mounted in eccentrics to provide a variable gap spacing. There were two problems inherent with this arrangement. It was difficult to access the rolls for either photographic observations or manual adjustments. Secondly, the replacement of the rolls required a complete dismantling of the system. Since the project required close visual observation of the nip, frequent adjustments to the pressure transducer and its related components, and the use of several types of roll surfaces, the system was redesigned with the rolls attached in a cantilever fashion (Fig. 9). The shafts are permanently mounted in the bearings, and the rolls are removable. The interior of the rolls are open on the nonattached side to allow easy access.

Several other modifications were made to the test apparatus and include: remote control of the scraper blades and timing mechanism, an adjustable dam to control the fluid level in the tray, a heat exchanger and recirculating pump to control the fluid temperature and motion through the system.

PRESSURE MEASUREMENTS

To obtain pressure measurements within the nip, a small pressure transducer was embedded in the surface of the applicator roll (Fig. 10). The pressure sensitive diaphragm was positioned approximately one-quarter of an inch from the outer surface of the roll and was exposed to the surface via two small 0.012-inch diameter holes (located parallel to the roll axis). The two holes were needed in order to insert the fluid without removing the pressure transducer.

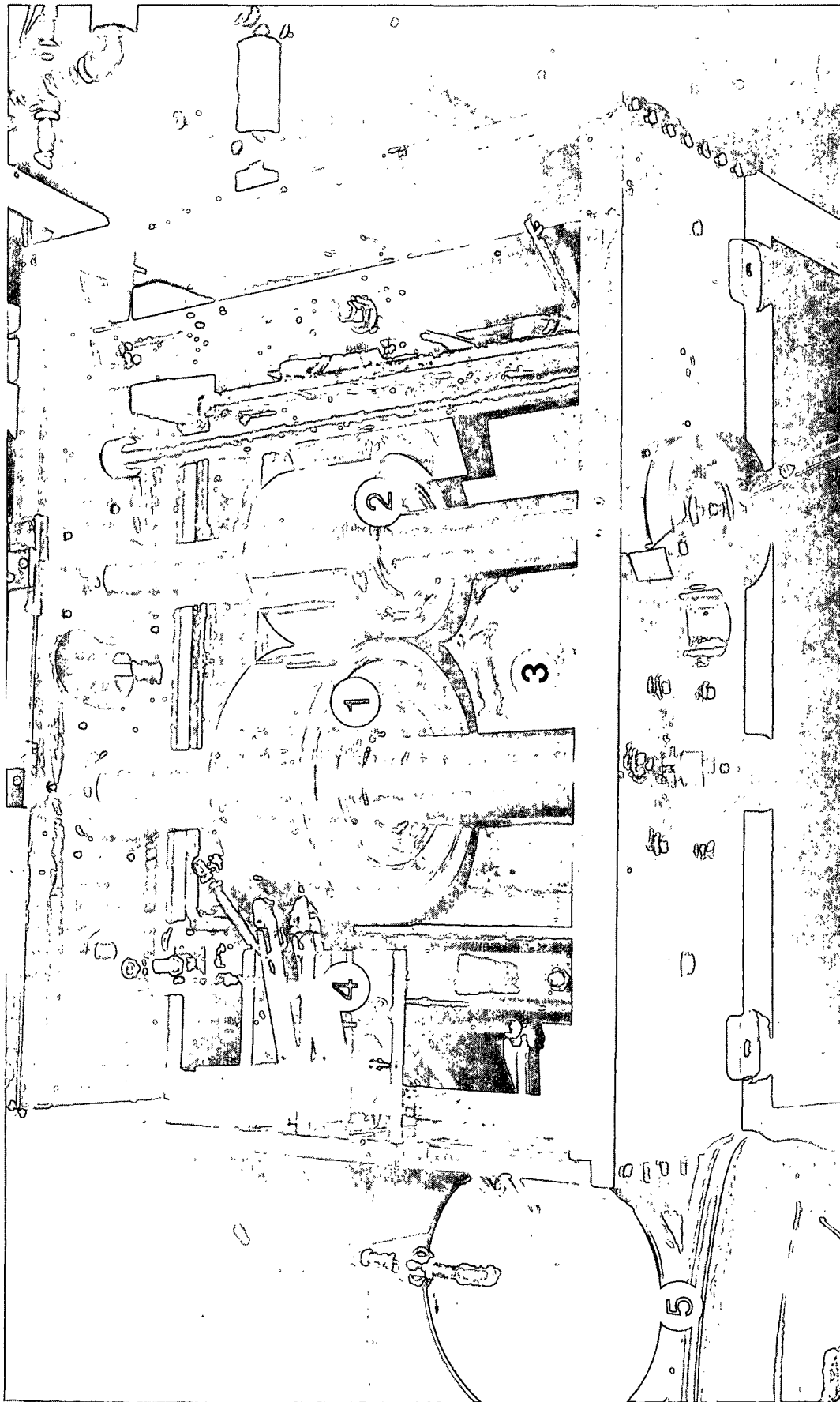


Figure 8. Experimental Applicator System

1. Applicator Roll; 2. Metering Roll; 3. Adhesive Tray;
4. Scraper Blade and Assembly; 5. Scale and Collection Pan

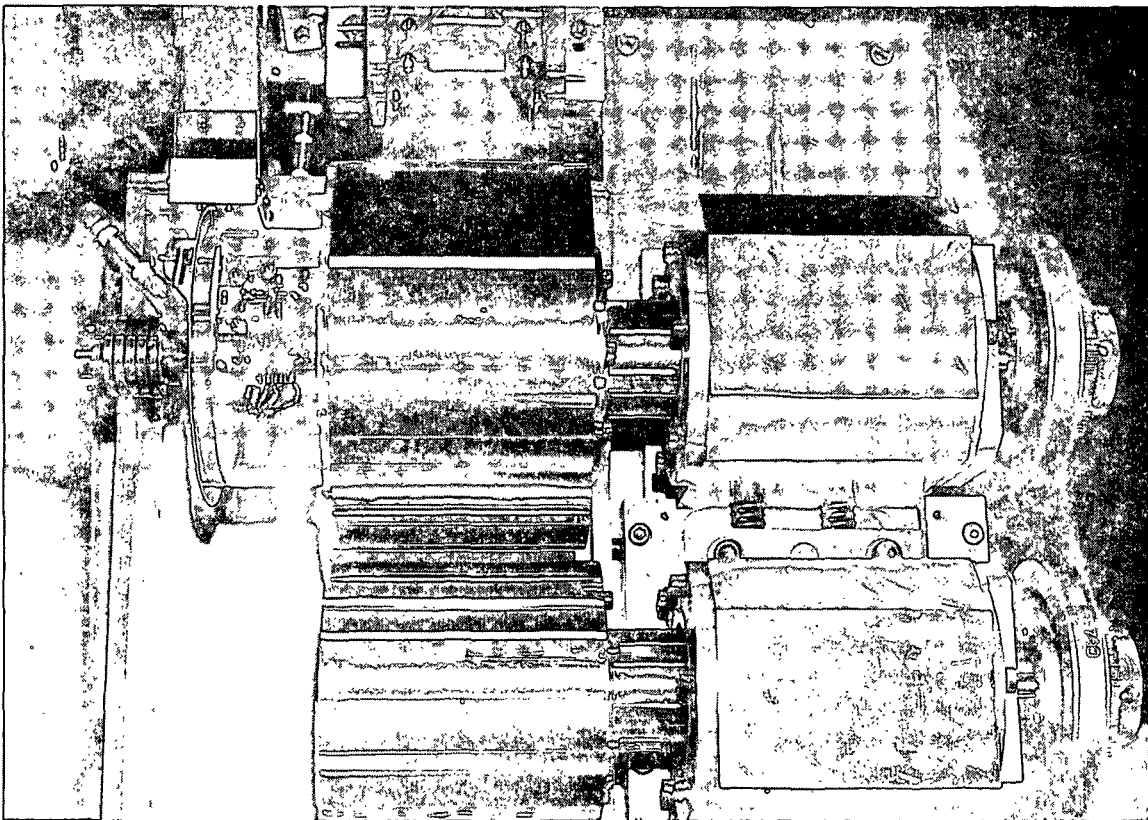
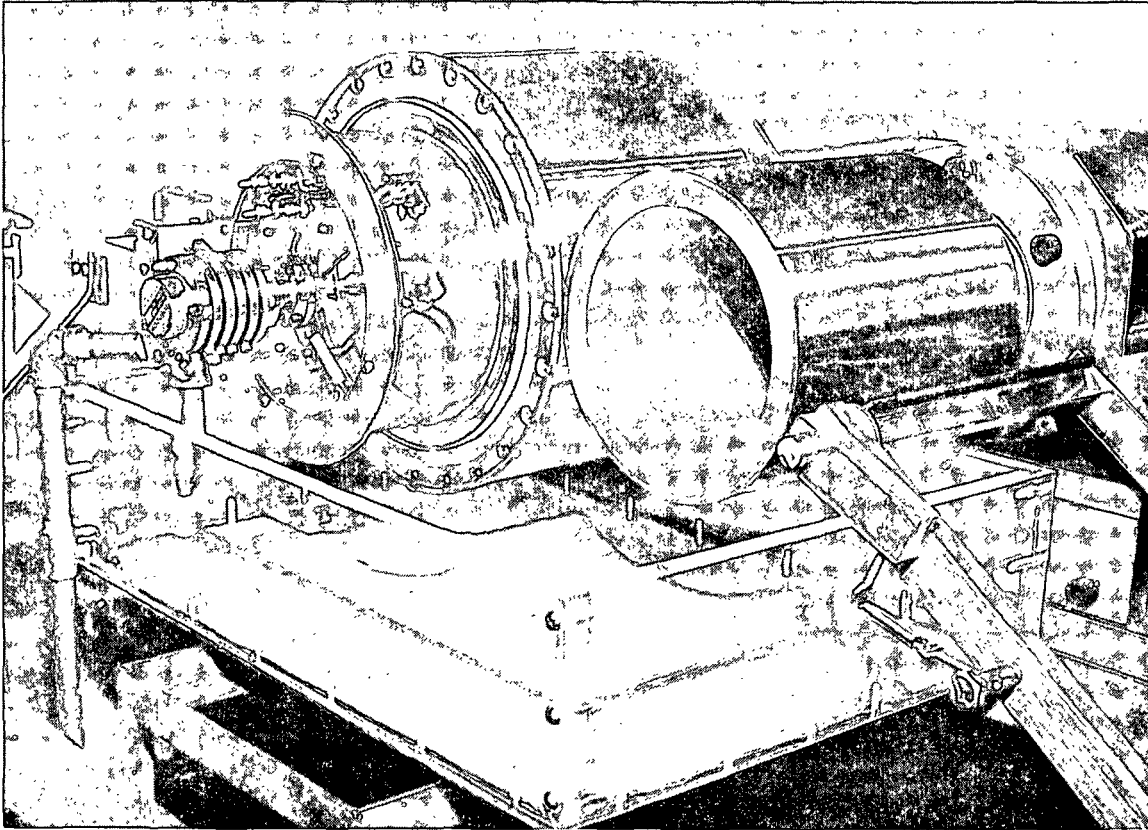


Figure 9. Rebuilt Adhesive Applicator (Side View and Top View)

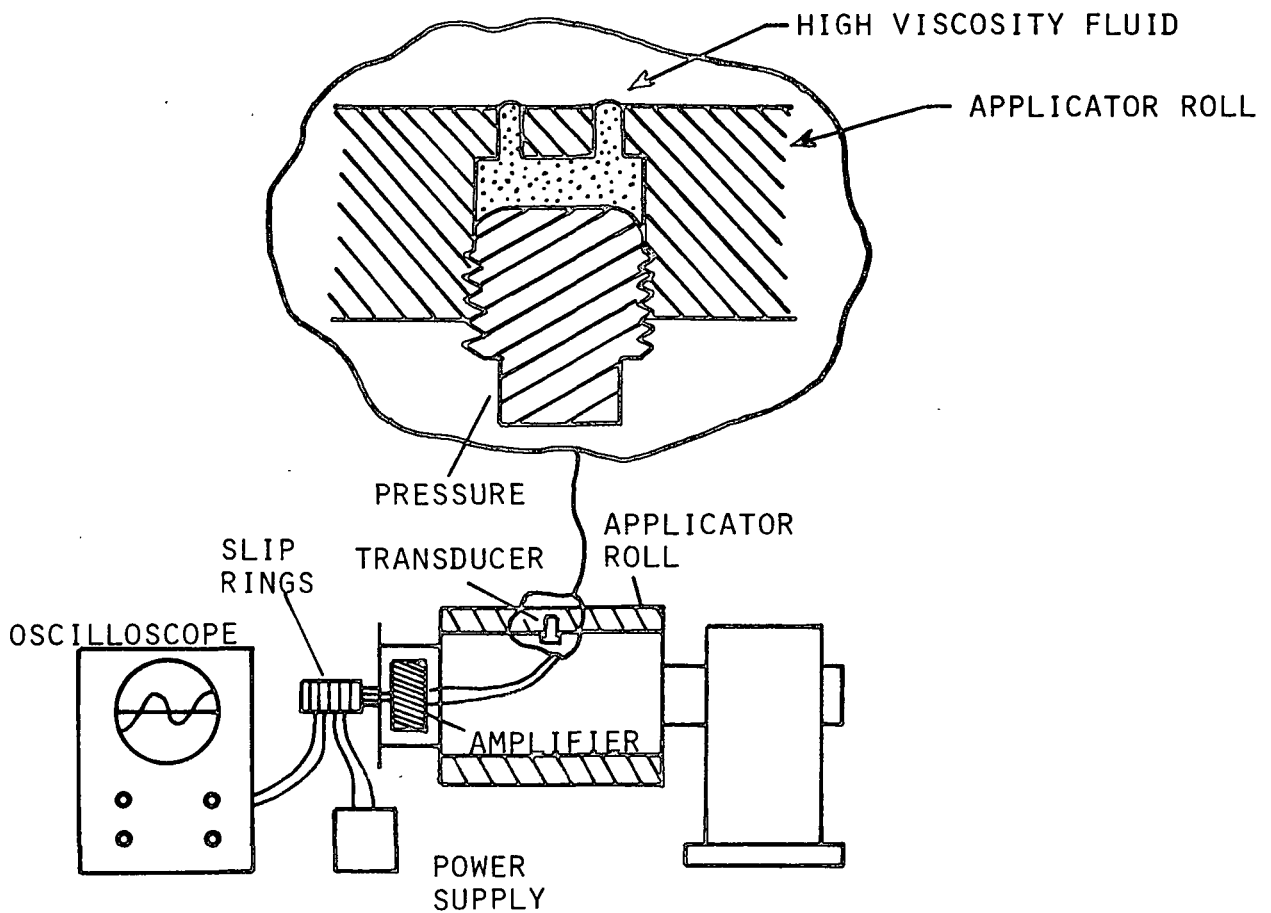


Figure 10. Pressure Monitoring Apparatus

The volume between the probe and the outer surface was filled with a high viscosity fluid to transmit the pressure pulse and to prevent the fluid from being thrown from the roll by the centrifugal forces experienced at high speeds. Also, the high viscosity fluid prevented air bubbles from being entrapped in the small ports. Air bubbles were trapped in the ports when water was used as the pressure fluid, and it caused the pulse to oscillate severely after the fluid separated from the metering roll.

The pressure transducer (Pitran PT-22) was designed to produce a 1 v/psi signal. The output signal was amplified and displayed on an oscilloscope. The

amplifier was physically mounted in a cylindrical cover attached to the open end of the roll. The output was then channeled through mercury slip rings and finally to the oscilloscope. Continuous direct current power was supplied to the amplifier via the slip rings.

In order to define the location of the pressure probe, a photocell and slotted disk were utilized as shown in Fig. 11. The initial slot opening is positioned so that the pressure transducer circuitry is opened about 2 inches before the mid-nip. The entire pulse width is about 2-1/2 inches, and the slotted disk could be adjusted to obtain the pressure measurement at various locations within the nip.

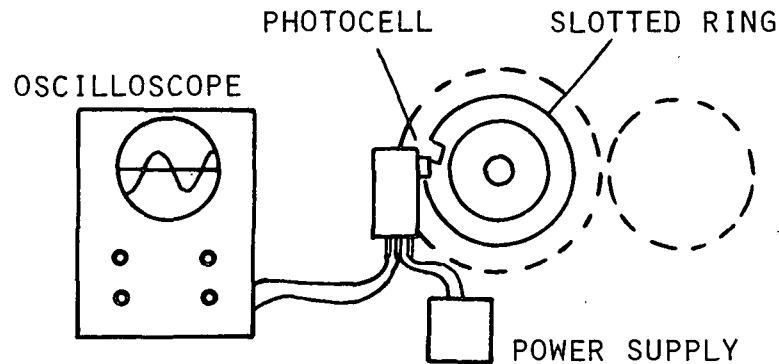


Figure 11. Oscilloscope Triggering Apparatus

The pressure transducer was calibrated statically. Then the gap spacing between the rolls and the desired operating speeds for the rolls were set. The oscilloscope was adjusted to obtain a clear and full width trace of the pressure distribution (the magnitude of the pulse was not adjusted). A series of photographs were taken for various operating conditions while the scope settings remained fixed. Some typical pulses are shown in Fig. 12 and 13.

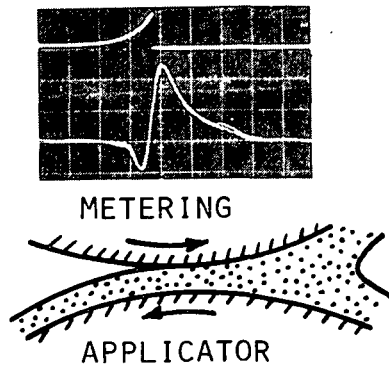


Figure 12. Oscilloscope Trace of the Pressure Distribution

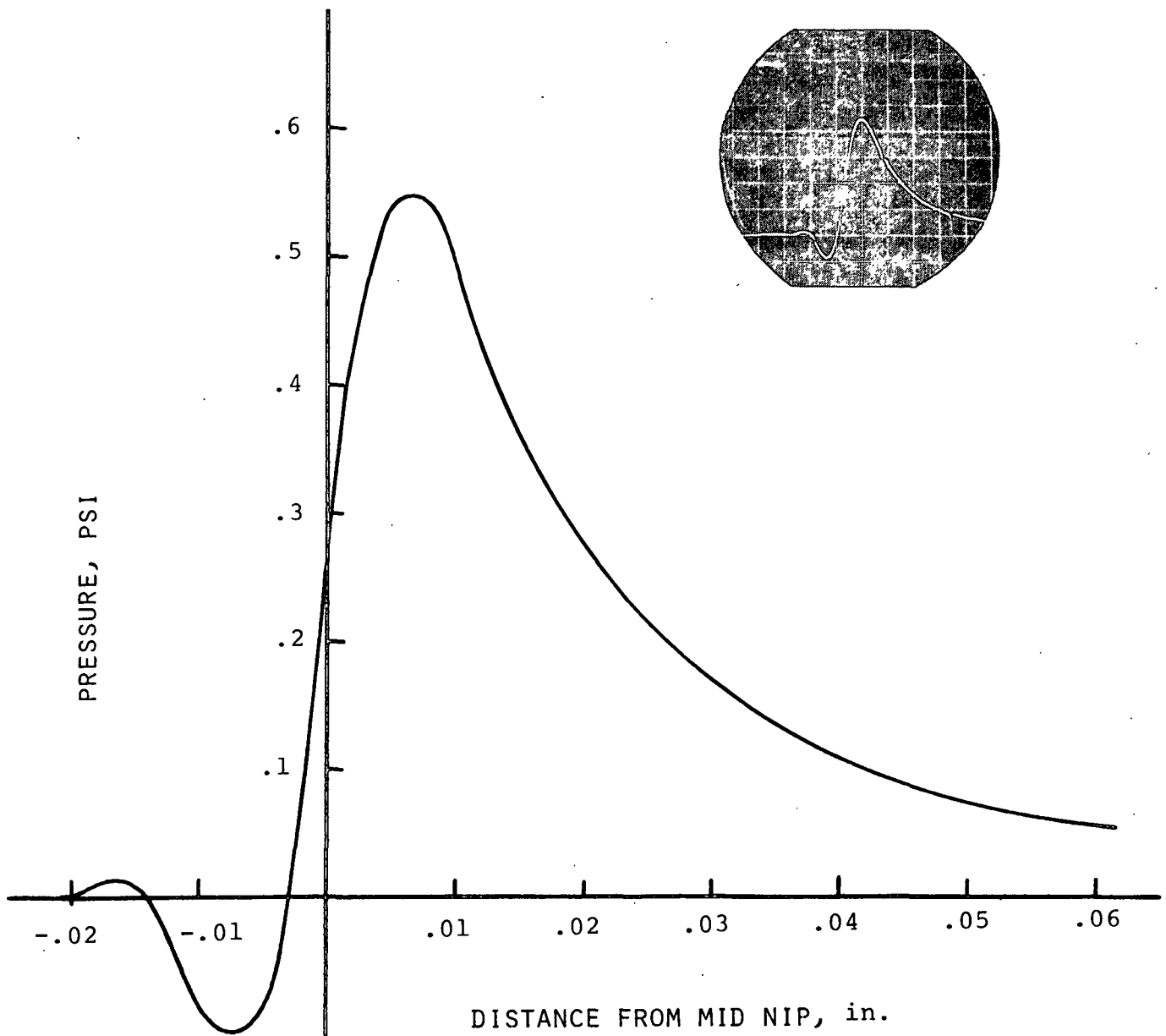


Figure 13. Typical Pressure Distribution

The data obtained in this manner is somewhat ambiguous since the amount of fluid picked up by the applicator roll and forced into the nip varies. This variation affects the magnitude and shape of the pressure distribution. Therefore, our future plans include taking a statistical average of many pulses in order to better define a particular operating condition.

PHOTOGRAPHS OF SURFACE PHENOMENA

In order to describe and bound the various surface phenomena that occur on the surface of the applicator roll, a photographic history was taken for various operating conditions and consistencies of the adhesives. A 35 mm camera was used with a flash attachment, the camera facing down upon the surface of the roll. These photographs were made before the new system was reconstructed. As a result, the pictures are of the surface on the only roll available at that time. The roll was approximately 18-inches long and made of ground steel with the same diameters as conventional equipment (applicator roll 10-inch diameter; meter roll 6-inch diameter). The roll also has finger slots engraved around the circumference at the normal intervals of approximately 2 inches.

RESULTS

PRESSURE MEASUREMENTS

Pressure measurements were obtained using Polybutene No. 6 as a working fluid. Typical pressure distributions are shown in Fig. 12 and 13. The upper oscilloscope trace in Fig. 12 marks the mid-nip location. The pressure pulse builds up gradually as the fluid is squeezed between the rolls, and a maximum pressure is reached just before the mid-nip. The fluid separation from the metering roll occurs very near the mid-nip or slightly above mid-nip for the conditions shown in Fig. 12 and 13. However, later in this discussion it will be shown that the separation point moves within the nip depending upon the operating conditions. (Recall that the point of fluid separation from the metering roll may be approximated by the location of the pressure distribution.) After the fluid separates, the pressure becomes slightly negative due to the sudden release of pressure and relaxation of the film to a uniform thickness and velocity equal to the surface speed of the applicator roll. The length of the pressure pulses depends upon the operating conditions and seemed to vary between 1/4 and 3/4 inch. The magnitude of the maximum pressures ranged from an undetectable signal (less than 0.1 psi) to approximately 1.5 psi.

The pressure distributions obtained for Polybutene No. 6 were converted into information to be used in completing the analytical model for film thickness on the applicator roll. Recall that the two parameters of interest were \underline{h}_m , the gap spacing between the rolls, and \underline{t} , the time the fluid is sheared. The gap spacing between the rolls can be estimated by using the distance between the mid-nip and the location of the point of maximum pressure. This information is plotted in Fig. 14 and 15 along with magnitude of the maximum pressures at

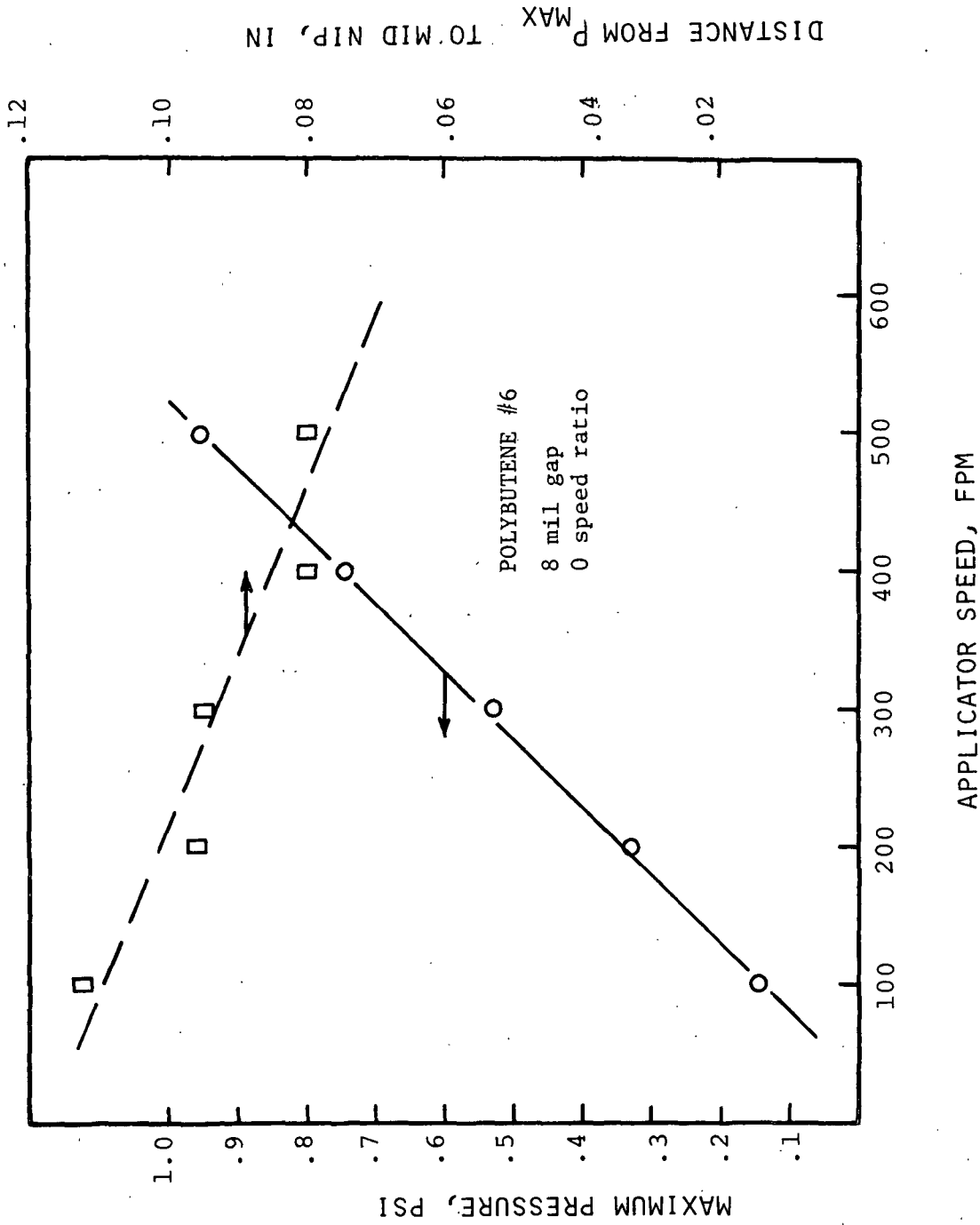
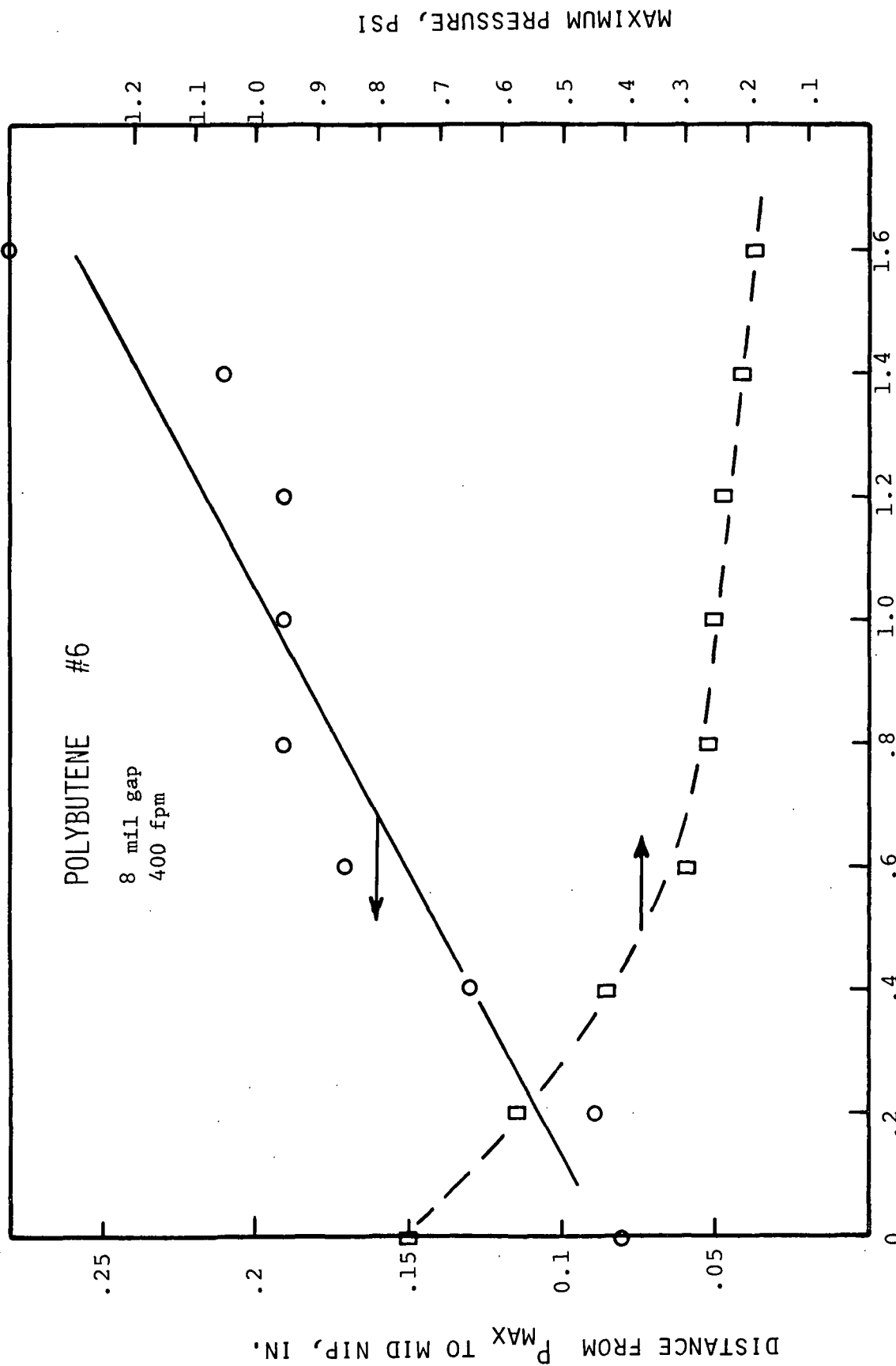


Figure 14. Maximum Pressure and Location vs. Applicator Speed



SPEED RATIO, METERING/APPLICATOR

Figure 15. Maximum Pressure AND Location vs. Speed Ratio

various speeds and speed ratios. In both figures, there is little scatter to the maximum pressure data. The maximum pressure linearly increases with speed. Initially, the pressure drops with speed ratio and eventually becomes nearly constant at speed ratios larger than 0.8.

The measurement of the distance between the point of maximum pressure and the mid-nip location was less accurate since the location of the maximum pressure and mid-nip are difficult to visually estimate from a photograph of an oscilloscope trace. This is evident in the scattered data shown in Fig. 14 and 15. The distance between the mid-nip and maximum pressure increases uniformly with speed ratio and it decreases with speed. One of the unexpected results of the experiment was the linear relationship between the magnitude of the peak pressure pulse and speed. It was presupposed that this relationship would be quadratic following a Bernoulli type equation. The linear curve implies that more than simple momentum transfer occurs or that the pickup conditions which control the amount of fluid forced into the nip are strongly influenced by the applicator speed.

The shearing time, t_s , was to be estimated from the point of maximum slope to the mid-nip. However, the photographs are not detailed enough for these points to be estimated with any precision. Also, as was stated earlier, there was some fluctuation in the pulses which made this type of measurement much too uncertain. Better measurements could be obtained by taking many samples and statistically averaging them.

Additionally, two other obstacles made it debatable the shearing time would ever be a meaningful quantity to estimate. First, from observations of pressure pulses at various speed ratios (see Fig. 16) the shearing time is

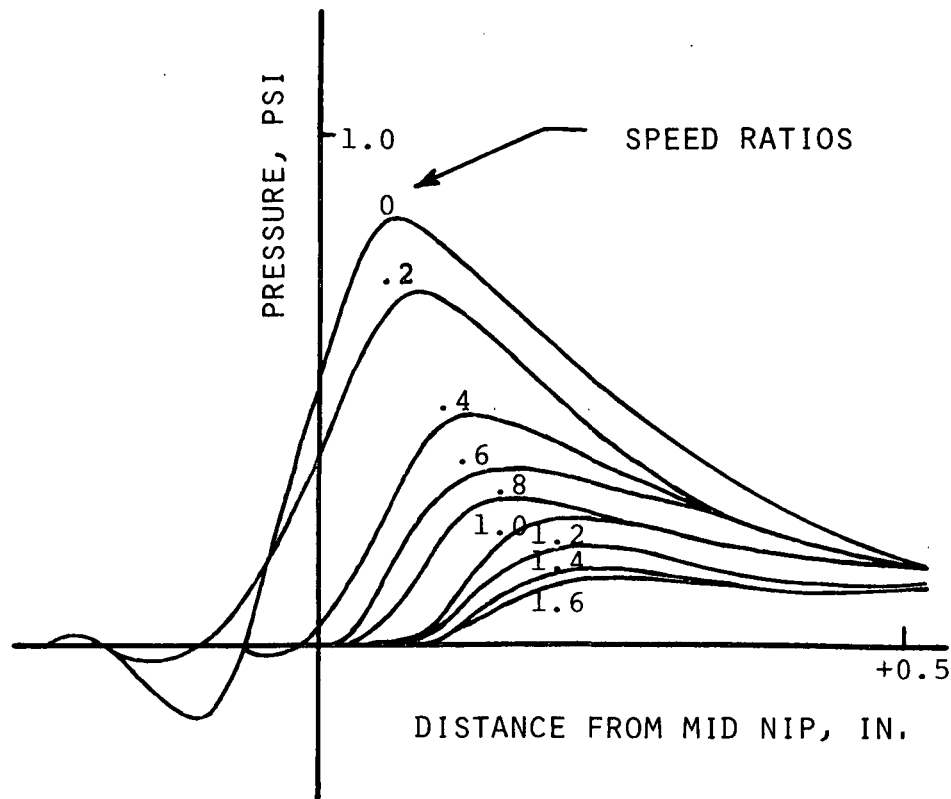


Figure 16. Development of the Pressure Pulse with the Speed Ratio

extremely small and almost impossible to measure. However, the spatial resolution of the distance limits the measurement of the time, and since the holes in the roll are already 0.01 inch there is little hope of improving the time measurement. It appears that the time information is too sensitive to be used in the analytical model. Secondly, the separation point from the metering roll moves in and out of the mid-nip, depending upon the speed ratio. Recall that the separation point can be estimated by the point of maximum gradient on the pressure distribution. At speed ratios of 0 and 0.2 the fluid separates from the metering roll above the nip, and this violates the assumption made in the analytical model. For the other ratios, separation occurs below the nip.

The movement of the separation point in and out of the nip was conjectured in Report One as the cause of the crossover point of the constant speed lines as shown in Fig. 2. The reversal in the magnitude of the film thickness was attributed to the reverse affects of fluid pressure when separation occurs on either side of the nip. This hypothesis is supported by the data shown in Fig. 16. The fluid separates above the mid-nip for speed ratios of 0 and 0.2; and at a speed ratio of approximately 0.4, separation occurs at mid-nip. On the film thickness curve for Polybutene No. 6 (Fig. 17), the crossover is between 0.4 and 0.6. Therefore, there seems to be some correlation between the two occurrences.

One other noteworthy feature of Fig. 16 is how the separation point moves below the nip with increasing speed ratio. After the speed ratio is increased over 1.0 there appears to be little movement of the separation point. This occurs because at these speed ratios the distance of the separation point below the nip is approximately 0.1 inch. At this location the gap spacing between the rolls has increased by almost 50%. The unwetted surface of the metering roll cannot move farther within the nip without being wetted by the fluid, and the separation point remains nearly constant. The values of the speed ratios where there is little movement of the separation point seem to coincide with the speed ratios where the film thickness curves level out (Fig. 16 and 17).

A similar argument may be offered to explain the film thickness variations in film that occur for different degrees of wiping of the metering roll. A thin film of fluid on the metering roll will draw the separation point above the mid-nip, and the film thickness characteristics will be completely different from the case when the metering roll is wiped clean and the fluid separates below the mid-nip.

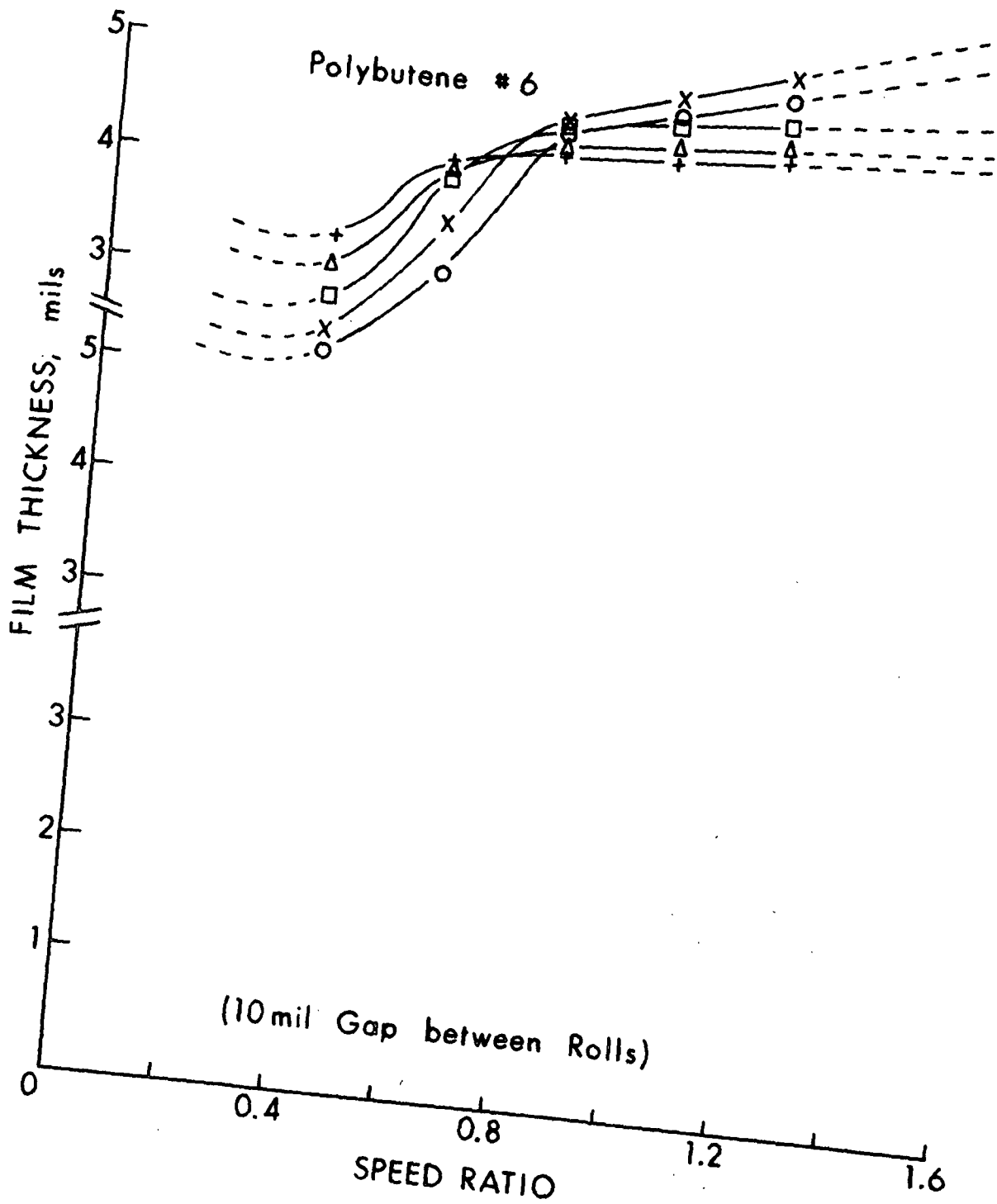


Figure 17. Film Thickness Versus Speed Ratio

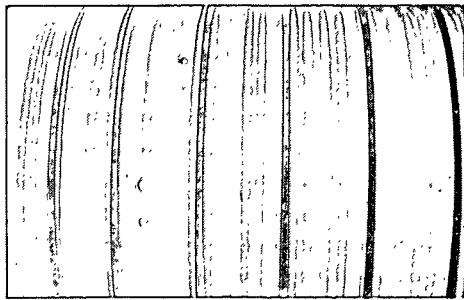
FILM STABILITY PHOTOGRAPHS

Photographs of the applicator roll surface were taken with four adhesives ranging in solids content from 20 to 26%. The speeds varied from 50 to 700 fpm (surface speed) and the ratios ranged from 0 to 1.6. Selected photographs (see Fig. 18-20) display the changes that occur in the film surface conditions on the applicator roll. The dark divisions on the roll are the finger slots.

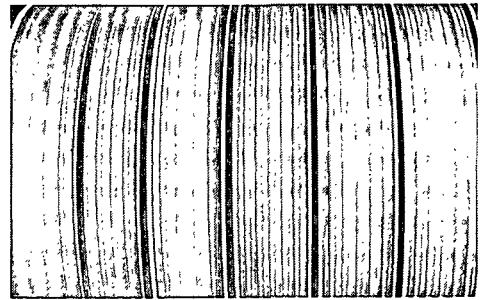
The progressive development of the "ringing" instability is clearly seen in Fig. 18. As the applicator speed is increased, the number of rings per unit width increase, the rings become more distinct, and the height of the individual rings from the roll surface is diminished. Although it is not clearly evident in Fig. 18, the data show that the rings become more pronounced at high applicator roll speeds and low metering roll speeds, i.e., low speed ratios.

The data in Fig. 19 is more representative of typical operating ranges. The applicator roll is set at 500 fpm and the speed ratio increases from 0 to 750 fpm (speed ratio range of 0 to 1.5). Again, a 20% solids adhesive is shown. As the speed ratio is increased, the ring patterns gradually disappear and are almost undetectable at a speed ratio of 0.2. From speed ratios of 0.2 to 1.0, which covers the normal commercial operating range, the film is very uniform. At higher speed ratios (1.0 to 1.5), the film appears to be rough, almost as if it were in turbulent motion.

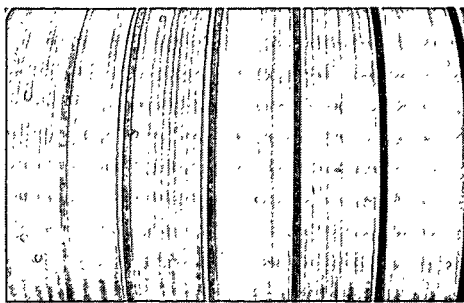
Figure 20 displays the effect of changes in solids content on the film. Increasing solids content increases the adhesive viscosity at both high and low shear rates (Table I). The viscosity changes are much larger for the low shear



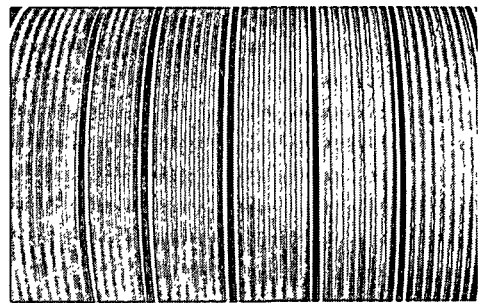
50



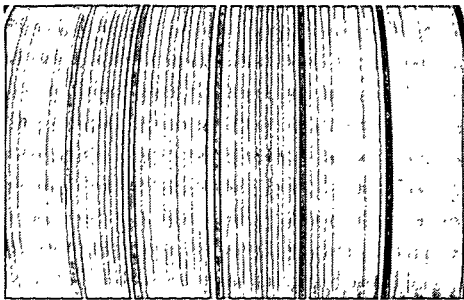
400



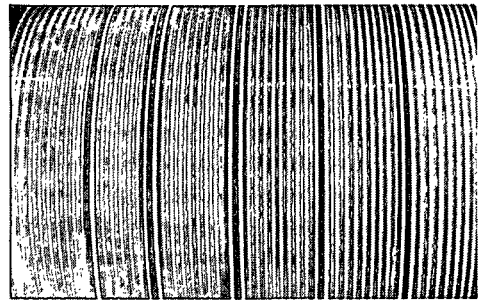
100



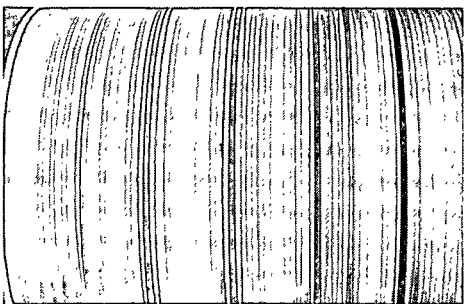
500



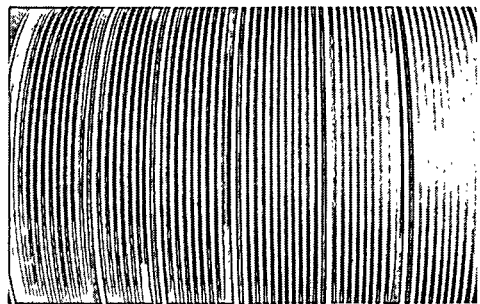
200



600

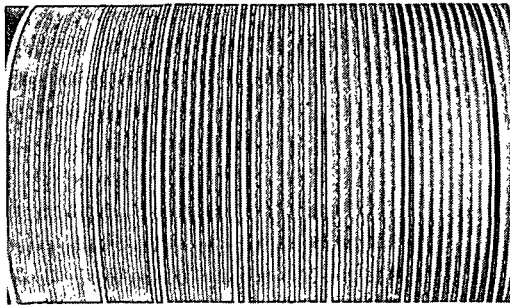


300

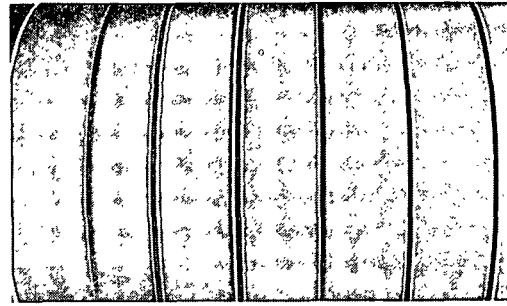


700

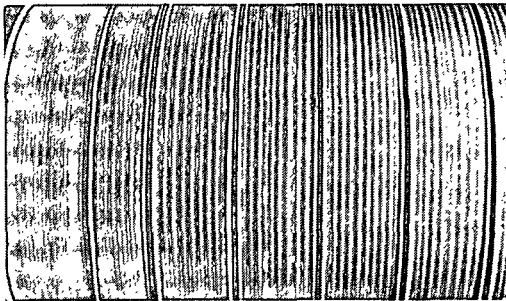
Figure 18. Ring Development with Applicator Roll Speed in fpm (Speed Ratio = 0, 20% Solids)



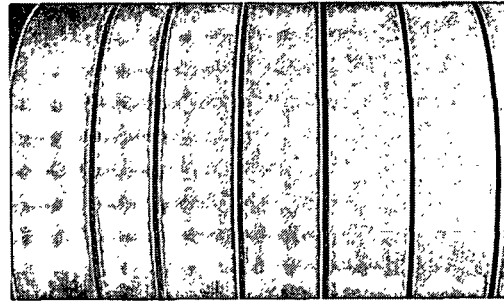
0



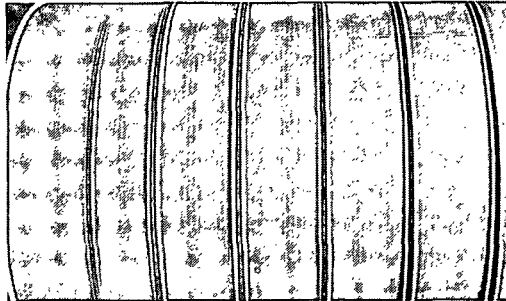
250



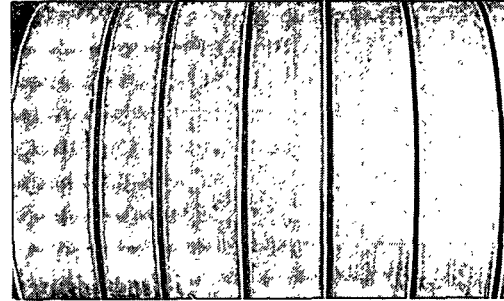
25



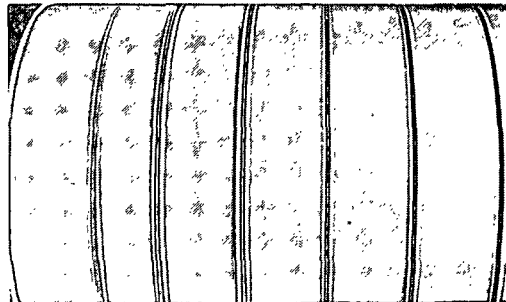
500



50



750

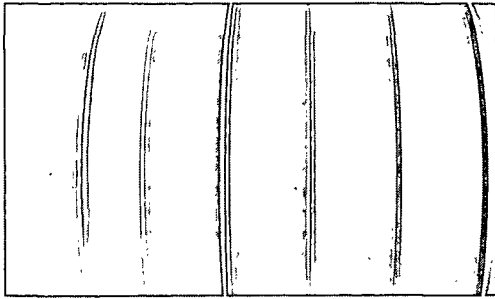


100

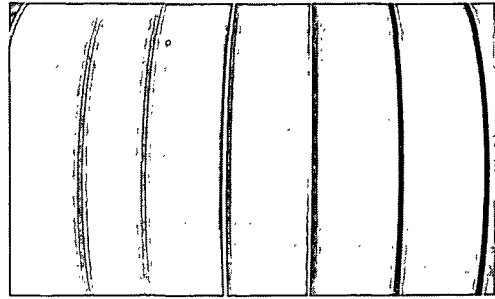
Figure 19. Film Surfaces with Metering Roll Speed in fpm (Applicator Roll = 500 fpm, 20% Solids)

metering 50
applicator 100

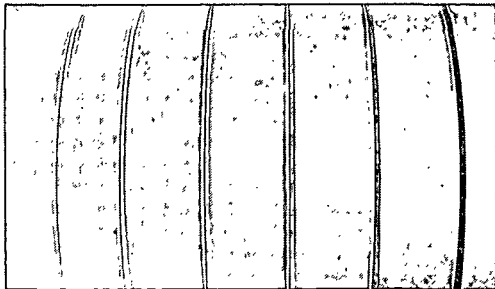
metering 250
applicator 400



20%



20%



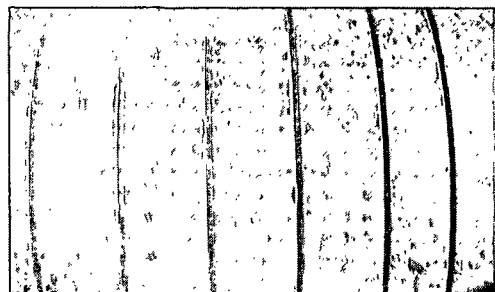
22%



22%



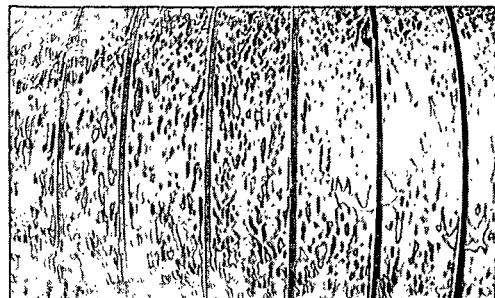
24%



24%



26%



26%

Figure 20. Film Surfaces with % Solids

rates. This is consistent with the Hercules viscometer rheograms described in Report One.

TABLE I
COMPARISON OF HIGH AND LOW SHEAR VISCOSITIES

Solids Content, %	High Shear Viscosity, cp	Low Shear Viscosity (Stein-Hall sec)
20	~28	35
22	~30	60
24	~35	108
26	~45	Off scale

Two typical operating conditions (applicator roll = 100, speed ratio 0.5, and applicator roll = 400, speed ratio 0.625) are displayed for increasing solids content. A gradual deterioration of the surface film is clearly observed with increasing solids. For the conditions studied photographically, the complete roll "stripping" was not observed. However, "stripping" did occur at speed ratios larger than the test conditions but only for the 24 and 26% solids content adhesives.

The information on Fig. 18-20, suggests that the normal operating conditions for adhesive applicators are nearly optimum on a reverse roll device from the standpoint of surface phenomena. The ringing seems to be associated with very low speed ratios ($0 \sim 0.2$). The "blotching" and "stripping" do not appear under normal operating conditions (approximate speed 100-600 fpm; approximate speed ratio 0.3-1.0) except for higher percent solid adhesives.

"Ringing" appears to be a surface condition distinct from "blotching" and "stripping" and directly related to the nip conditions. The rings seem to be a function of the nip conditions. In particular, they seem to be related

to large fluid pressure below the nip, which at low speed ratios is sufficient to force the fluid to separate from the metering roll above the mid-nip. At increased speed ratios, the separation point is drawn below the mid-nip, and the rings disappear. The similarities of pressure distribution data and the "ringing" seem to indicate that the "rings" are primarily an effect of the mechanics of the applicator rather than being fluid property dependent.

On the other hand, the photographic information for the other surface phenomena, "blotching" and "stripping", implies that the two are related and that "stripping" is a severe form of the "blotch" patterns. The phenomena are more complex than "ringing" instability in that they appear to be intimately dependent upon the fluid properties and roll surface properties as well as the operating conditions of the adhesive applicator. Therefore, a much more comprehensive investigation would be required to fully define the phenomena.

ANALYTICAL MODELS.

FILM THICKNESS PREDICTION

The analytical model for predicting the film thickness on the applicator roll for various operating conditions was derived in Report One and reviewed in the Introduction Section - Film Instabilities. The final form of the model was given in Equation (1) as

$$\delta_a = (1 - u_m/u_a) h_m/2 + 4/\pi^2 (1 + u_m/u_a) h_m e^{-\pi^2 vt/h_m^2} \quad (1)$$

The two quantities required for the determination of δ_a are $\underline{h_m}$ and \underline{t} . They are to be obtained from the pressure distribution. The equation may be simplified by using

$$SR = u_m/u_a$$

and

$$K = \pi^2 vt/h_m^2$$

Equation (1) becomes

$$\delta_a = h_m/2 [(1 - SR) + 8/\pi^2 (1 + SR) e^{-k}] \quad (2)$$

The value of $\underline{h_m}$ can be determined from the value of $\underline{x_m}$ given in Fig. 14 and 15. The value of $\underline{h_m}$ is a quadratic function of $\underline{x_m}$ and is given by

$$h_m = h_o + r_a + r_d (r_a^2 - x_m^2)^{1/2} - (r_d^2 - x_m^2)^{1/2}, \quad (3)$$

where $\underline{r_a}$ = radius of applicator roll

$\underline{r_d}$ = radius of doctor roll

This function is plotted in Fig. 21. The remaining unknown quantity is the shearing time \underline{t} in the exponent, \underline{k} . Since the value of \underline{t} could not be

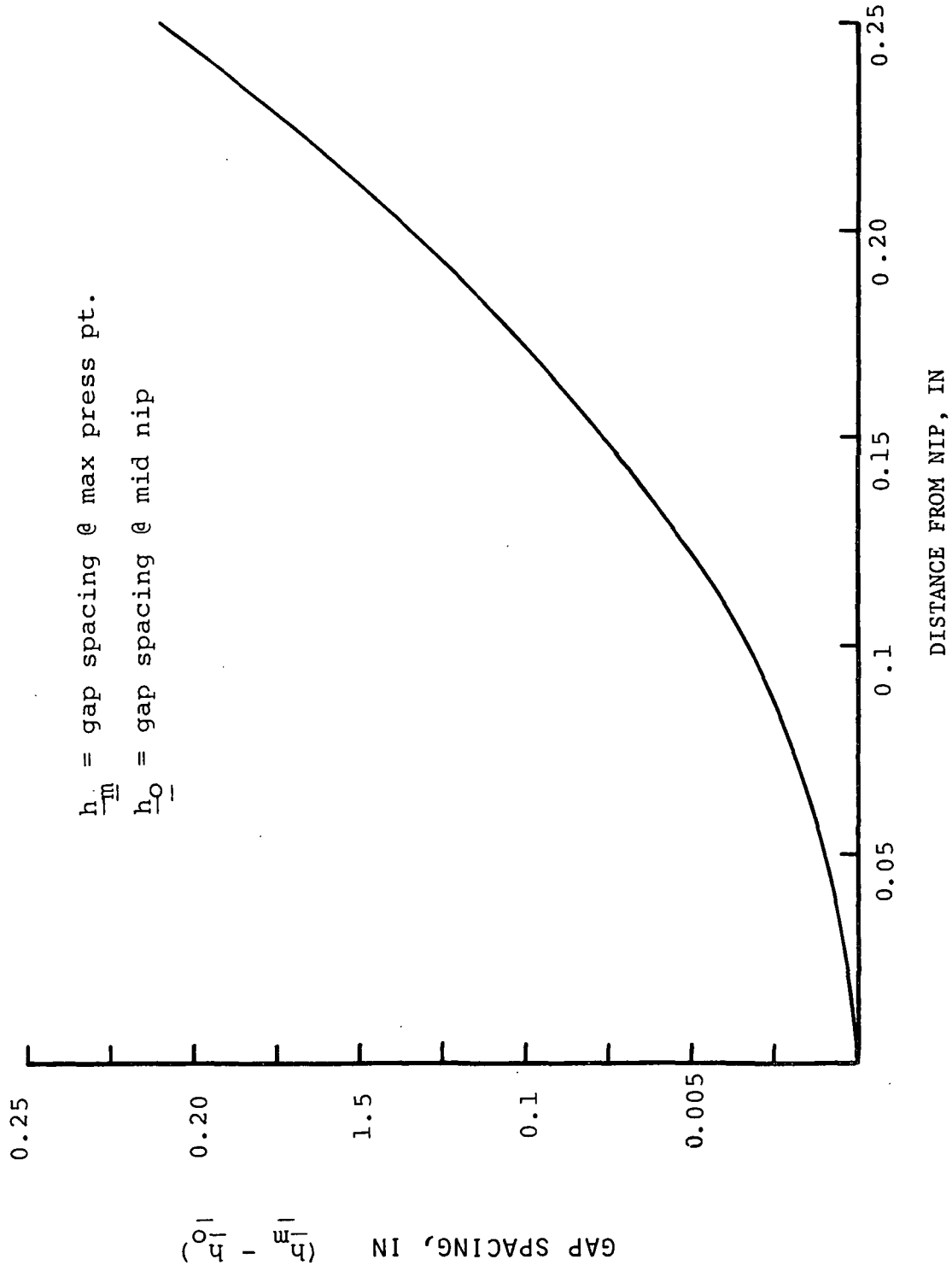


Figure 21. Gap Spacing vs. the Distance from the Nip

estimated with the limited amount of pressure information obtained for Polybutene No. 6, a reverse calculation was made using known values of δ_a to determine the values of k needed to duplicate the experimental curve (Fig. 17). The results of this calculation are shown in Table II.

TABLE II
ANALYTICAL CALCULATIONS FOR POLYBUTENE NO. 6

Speed	Speed Ratio	$\frac{h}{m}$, inch	δ_{exp} , inch	e^{-k}
100	0.0	0.0112	0.0032	0
200	0.0	0.0107	0.0036	0
300	0.0	0.0103	0.0035	0
400	0.0	0.0099	0.0037	0
400	0.2	0.0111	0.0022	0
400	0.4	0.0126	0.0022	0
400	0.6	0.0142	0.0032	2.709×10^{-6}
400	0.8	0.0162	0.0036	2.137×10^{-6}
400	1.0	0.0182	0.0036	1.157×10^{-6}
400	1.2	0.0208	0.0037	1.484×10^{-6}
400	1.4	0.0232	0.0038	1.612×10^{-6}
400	1.6	0.262	0.0038	1.856×10^{-6}
500	0.0	0.0096	0.0038	0

In nearly half of the operating conditions, the value of k is too small to be meaningful.

The inability to obtain values for k lie in the sensitivity of Equation (2) to values of t and the inability to obtain extremely precise measurements of t and x_s . The precision of the measurements is basically controlled by the size of the probe surface. A spatial resolution of 0.012 inch is approaching the practical limits of pressure measurements. Therefore it seems improbable that improved measurements of t and x_s can be made. This suggests

that the only alternative may be to use regression analysis to statistically determine a relationship to predict the film thickness δ as a function of operating variables.

Although the usefulness of the model presented in Report One seems limited, several aspects must be considered before it is dropped completely. First, these conclusions are based on a limited amount of information for the pressure distributions as well as the film thickness. Secondly, the comparison is based on pressure measurements obtained with a ground stainless steel roll and film thickness measurements made with a polished steel roll. There is an obvious effect of roll surface on the film thickness metered onto the applicator roll as was demonstrated by Jaeger (3). Finally, the limited pressure measurements were recorded photographically and do not provide adequate spatial resolution to make precise measurements of \underline{x}_m , \underline{x}_s , and \underline{t} . Statistically average data may provide improved values for these quantities. Also, they will be more consistent with the film thickness measurements, which are averaged values.

MODELING SURFACE PHENOMENA

As was mentioned in Results - Film Stability Photographs, the "blotching" and "stripping" phenomena seem to be complex functions of the fluid and roll surface properties as well as the operating conditions. Therefore, with the limited amount of variables observed, it is unlikely that a complete description of the phenomena including a nondimensional scaling factor can be determined. However, from experimental experience it seems likely that these phenomena may have their origins at the pickup location under the applicator roll. Here the roll roughness, viscosity of the fluid, and applicator roll speed may be such that the fluid does not sufficiently wet the roll, and clean areas exist as the fluid is forced into the nip.

On the other hand, the "ringing" phenomenon seems to have its origins in the mechanics of the system and can possibly be defined by a scaling factor. Initially it was believed that this form of instability was associated with the development of a secondary laminar flow perpendicular to the rotational motion of the rolls (radially outward). This type of flow instability was first investigated by Taylor (4) and is referred to as Taylor-Goertler vortex motion. The conditions for a flow to become unstable in this fashion are expressed with a characteristic Taylor number, Ta .

$$Ta = U_i d / \sigma \sqrt{d/R_i} \quad (4)$$

where d = gap width

R_i = inner radius

U_i = peripheral velocity of the inner cylinder

σ = kinematic viscosity

However, the value of the Taylor number for typical conditions ranges from about 0.1 to 10, and this is well below the critical Taylor number for the onset of the instability (41.5). If the fluid separates from the metering roll at a location where h is significantly larger than h_o , the Taylor number can increase by an order of magnitude, which brings it closer to the critical value. The fact that the geometry is not precisely the same as the concentric cylinders used in Taylor's experiment must also be considered. Therefore it is still possible that the "rings" can be a Taylor-Goertler instability.

The "ringing" phenomena may be alternately considered from a different approach as Yih and Kingman did (5). They developed a stability criterion for a fluid on a single rotating cylinder using a linearization of the Navier-Stokes equation. Their criterion was expressed in the form

$$K = 1/R \sqrt{1 + \rho\omega^2 R^2 / \sigma} \quad (5)$$

where \underline{K} = wavenumber of the rings

σ = surface tension of the fluid

The number of rings for the conditions investigated in the photographic portion of this work agree in the order of magnitude with Equation (5). It is possible that both the Taylor instability and the "Yih and Kingman" form of instability may be the origin of the rings on the applicator roll. However, the number of rings used in evaluating this later instability is based on experimental rolls which contained finger slots positioned 2 inches apart. End effects must be considered and were not. Therefore, verification will rest on experiments with a much wider roll.

The phenomena of Yih and Kingman may be approached from another method using a variational approach. Essentially the thin film on the roll surface must be in equilibrium with centrifugal and surface tension forces.

The energy of the fluid on the applicator roll will tend to a minimum value and this may be expressed functionally as:

$$U = E - T = \text{minimum}, \quad (6)$$

where \underline{E} = free surface energy

\underline{T} = kinetic energy

The effect of gravity is presumed small and is neglected. Also, it is assumed that no fluid is thrown from the roll, and the system is constrained to maintain a constant fluid volume.

The individual terms of Equation (6) are written in terms of the parameters shown in Fig. 22.

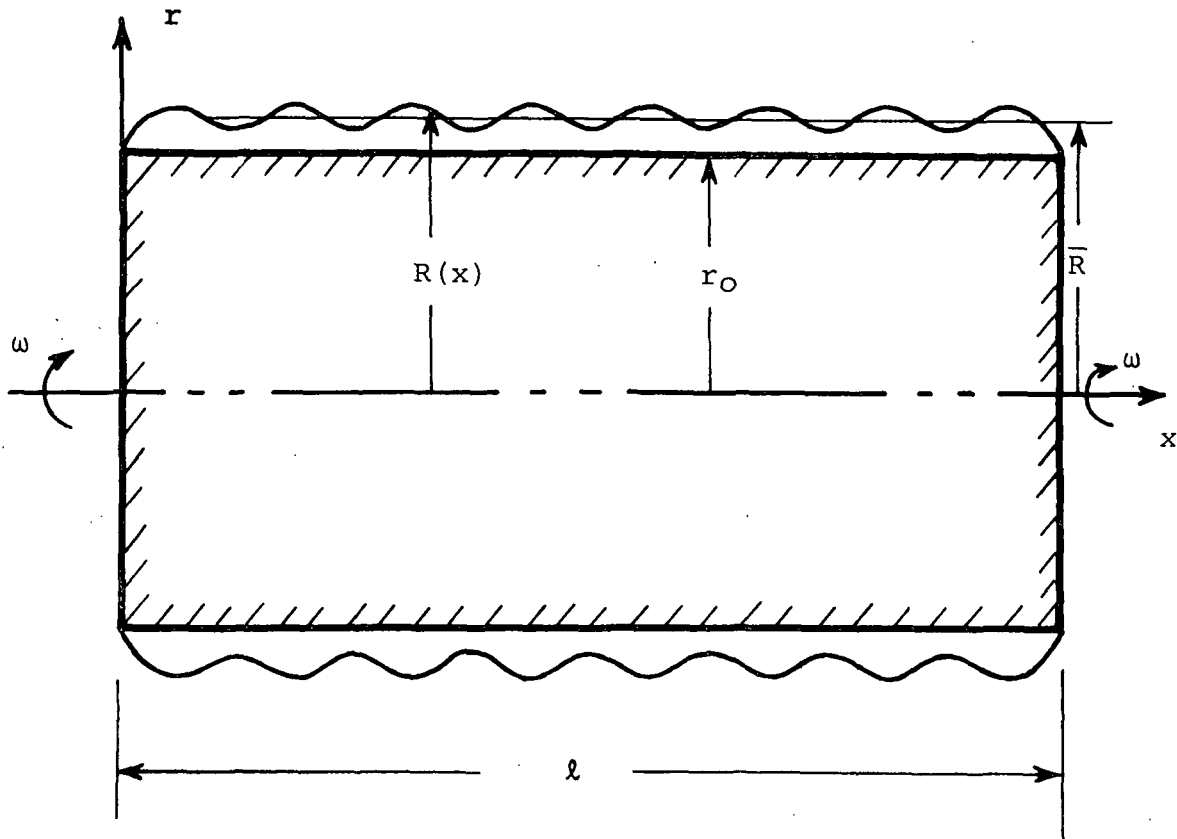


Figure 22. Ring Phenomena on a Free Roll

Free Surface Energy

$$E = \sigma S = 2 \pi \sigma \int_0^l R [1 + (dR/dx)^2]^{1/2} dx \quad (7)$$

Kinetic Energy

$$\begin{aligned} T &= 2 \pi \int_0^l \int_{r_0}^R (1/2 \rho \omega^2 r^2) dr dx \\ &= 1/4 \rho \omega^2 \pi \int_0^l (R^4 - r_0^4) dx, \end{aligned} \quad (8)$$

where σ = surface tension

ρ = fluid density

The volume constraint is expressed by

$$\begin{aligned}
 V &= 2 \pi \int_0^1 \int_{r_0}^R r \, dr \, dx \\
 &= \pi \int_0^1 (R^2 - r_0^2) \, dx = \text{constant} \quad (9)
 \end{aligned}$$

Using variational methods for finding the minimum energy state prescribed in Equation (6) is restated as:

$$\delta U = \delta (E - T + \lambda V) = 0, \quad (10)$$

where λ is the Lagrange multiplier. Substituting Equations (7), (8), and (9) into Equation (10) yields:

$$\begin{aligned}
 \delta U &= \delta \left\{ 2 \pi \sigma \int_0^1 R [1 + (dR/dx)^2]^{1/2} \, dx \right. \\
 &\quad - \rho \omega^2 \pi/4 \int_0^1 (R^4 - r_0^4) \, dx \\
 &\quad \left. + \lambda \pi \int_0^1 (R^2 - r_0^2) \, dx \right\} = 0 \quad (11)
 \end{aligned}$$

or

$$\begin{aligned}
 \delta U &= \delta \left[\int_0^1 \left\{ 2 \pi \sigma R [1 + (dR/dx)^2]^{1/2} \right. \right. \\
 &\quad \left. \left. - \rho \omega^2 \pi/4 (R^4 - r_0^4) + \lambda \pi (R^2 - r_0^2) \right\} \, dx \right] = 0 \quad (12)
 \end{aligned}$$

Mathematically, the problem is to find the extremum of the integral

$$\begin{aligned}
 \int_0^1 L \, dx &= \int_0^1 \left\{ 2 \pi \sigma R [1 + (dR/dx)^2]^{1/2} \right. \\
 &\quad \left. - \rho \omega^2 \pi/4 (R^4 - r_0^4) + \lambda \pi (R^2 - r_0^2) \right\} \, dx \quad (13)
 \end{aligned}$$

where L is called the Lagrangian. The necessary condition for an extremum is that the Lagrangian satisfies Euler's equation

$$d/dx (\partial L / \partial R') - \partial L / \partial R = 0, \quad (14)$$

where $R' = dR/dx$. Substituting the Lagrangian into Equation (14) produces the differential equation of the surface film.

$$2 \pi \sigma \{ [1 + (R')^2]^{1/2} - [(R')^2 + R R''] (1 + (R')^2)^{1/2} + R (R')^2 R'' [1 + (R')^2]^{-3/2} \} - \pi \rho \omega^2 R^3 + 2 \pi \lambda R = 0 \quad (15)$$

The trivial solution is $R = \bar{R}$ where \bar{R} is the average film thickness and substitution into Equation (15) yields,

$$2 \pi \sigma - \pi \rho \omega^2 \bar{R}^3 + 2 \pi \lambda \bar{R} = 0$$

or

$$\lambda = \rho \omega^2 \bar{R}^3 - 2 \sigma / 2 \bar{R} \quad (16)$$

After a particular linearization,

$$(R')^2 \ll 1, \quad (17)$$

which assumes that the amplitude of variations in the surface film are small compared to the wavelength of the oscillations, Equation (15) becomes

$$2 \pi \sigma (R R'' - 1) + \pi \omega^2 \rho R^3 - 2 \pi [\omega^2 \rho \bar{R}^3 - 2\sigma/2R] R = 0 \quad (18)$$

If the surface can be described with a periodic function,

$$R = \bar{R} + A \sin K x \quad (19)$$

where K is the wave number. If it is assumed that

$$A \ll R, \quad (20)$$

such that A^2 terms can be neglected, then Equation (18) reduces to:

$$-k^2 \sin K x + (\omega^2 \rho R^3 + \sigma/\sigma R^2) \sin K x = 0, \quad (21)$$

or the wave number \underline{K} is:

$$K = 1/R \sqrt{1 + \rho \omega^2 R^3 / \sigma} \quad (22)$$

This is the same relationship found by Yih and Kingman, but it is arrived at from a completely different viewpoint. It is physically more informative since it describes the mechanisms of the instability as being associated with a balance between the centrifugal and surface tension forces.

CONCLUSIONS AND SUGGESTIONS FOR FUTURE RESEARCH

PRESSURE MEASUREMENTS

The pressure measurements, although limited in number, have provided valuable information concerning the mechanism of the film splitting in the nip region. The magnitude, duration, and general character of the pressure distributions were defined, and the technique for obtaining good spatially resolved measurements in the complex flow geometry were demonstrated. More extensive measurements are required to describe the effects of different fluids on the pressure distributions.

Some improvements can be made to the data collecting technique. First, there is some variation from signal to signal due to different quantities of fluid being picked up and forced into the nip. In order to make the pressure measurements consistent with the experimental data for film thickness which is an averaged measurement, it is recommended that numerous pulses be taken and average distribution be generated. This can be accomplished quite easily with the Institute's Tracor Northern Signal Analyzer. A second addition to the present technique could be the measurement of the pressure distributions on the metering roll. These measurements would more accurately define the film separation point from the metering roll. The same type of device used on the applicator roll can be utilized.

ANALYTICAL MODEL FOR FILM THICKNESS

The small amount of x_{in} and t data was not sufficient to adequately define the analytical model. The sensitivity of film thickness to the exponential term of the model and the inability to obtain the extremely precise

measurements required to define the exponent were demonstrated. Together, they may indicate that the model cannot presently be used. An alternative, although less pleasing, solution would be to apply regression analyses to the data in order to determine an empirical relation between the film thickness and operating parameters.

FILM STABILITY PHOTOGRAPHS

The photographic study of the film instabilities indicate that for typical operating conditions the film surface phenomena are not a severe problem. The "rings" generally occur at low speed ratios (below 0.2) and/or at much higher speeds. Additionally the "ringing" seems to be more closely connected with the operating conditions of the applicator system rather than the fluid properties.

The other two phenomena appear to be different stages of the same surface condition. They did not occur under most typical operating conditions unless the solids content of the starch adhesive was high (about 24%). These types of phenomena are much more difficult to predict because of their equally important dependence on the adhesive properties, applicator operating conditions, and the roll surface roughness.

MODELING FILM INSTABILITIES

The "ringing" phenomenon, because of its stronger dependence on flow conditions, seems to be easier to analyze. However, there is still conjecture as to whether the instabilities are Taylor-Goerther vortices or Yih and Kingman instabilities, and it is possible that the two forms of instability may be

related. More information concerning the rings is needed before the real cause can be ascertained. This would consist of obtaining wave number information from a larger applicator roll where end effects are less significant. Additionally, more detailed information of the flow conditions is needed to obtain a realistic value for the Taylor number and a nondimensional scaling parameter for the phenomena.

SUGGESTIONS FOR FUTURE WORK

Although all of the objectives of the project have not been thoroughly answered, the understanding of the mechanics of the adhesive applicator have increased significantly. A multitude of areas not only related to adhesive application but also important to much of coating operations have been defined. But since the scope of this project is directed at adhesive application, the following recommendations are offered for continued research in this area.

1. The results of this report indicate that film surface phenomena are not critical problems with regard to adhesive application; although they may be serious problems in the coating process. Therefore, since emphasis of this project is on adhesive application and an important unanswered question concerning adhesive application is still the transfer process of adhesive from the applicator roll to the flute tips of the medium. It is recommended that the work now continue into Phase II of the project. The dropped topics, because of their more fundamental nature, should be addressed in other specific projects, some of which will be listed below.

2. Additional work of a more fundamental nature should consist of the following:
 - a. Define the effects of roll roughness on the average film thickness on the applicator roll.
 - b. Obtain extensive pressure measurements via the nip region using statistically averaged data from both rolls and interrelate this information with an interfacial description of the phenomena occurring at the film splitting zone.
 - c. Observe and define the film instabilities with a reduced number of variables. In particular, experimentally define the instabilities using fluids of well known and a well behaved rheological character.
 - d. Analytically describe the film splitting and surface instabilities from an interfacial perspective.

NOMENCLATURE

<u>A</u>	=	Roll radius
<u>E</u>	=	Free surface energy
<u>h</u>	=	Gap spacing between rolls
<u>K</u>	=	Wave number
<u>k</u>	=	Constant
<u>L</u>	=	Lagrangian
<u>l</u>	=	Roll width
<u>P</u>	=	Pressure
<u>R</u>	=	Roll radius
<u>r</u>	=	Roll radius
<u>SR</u>	=	Speed ratio
<u>T</u>	=	Kinetic energy
<u>t</u>	=	Time
<u>U</u>	=	Roll surface speed, energy functional
<u>u</u>	=	Roll surface speed
<u>V</u>	=	Volume
<u>x</u>	=	Vertical location within the nip

Subscripts

<u>a</u>	=	Applicator roll
<u>d</u>	=	Metering (doctor) roll
<u>m</u>	=	Maximum pressure, metering roll
<u>o</u>	=	mid-nip location
<u>s</u>	=	Film splitting location
1	=	Applicator roll
2	=	Metering roll

δ = Film thickness

λ = Lagrangian multiplier

ν = Kinematic viscosity

ρ = Density

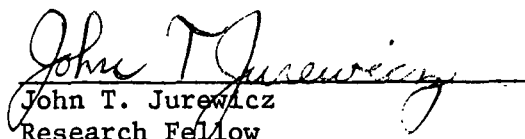
σ = Surface tension

ω = Angular velocity

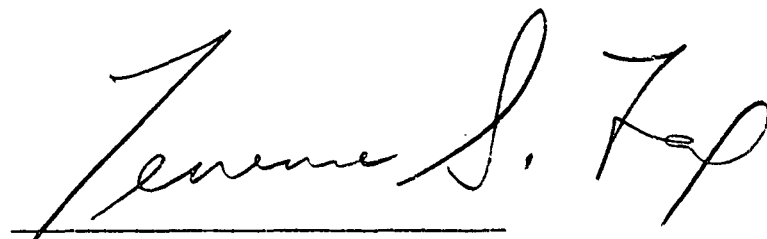
LITERATURE CITED

1. McKee, R. "Study of Bonding Potentials of Corrugated Medium," Project 2696-17, Report One, A Progress Report to FKI, Jan. 15, 1976.
2. Jurewicz, J. "A Study of Bonding Mechanisms of Corrugated Medium", Project 2696-17, Report One, A Progress Report to the Fourdrinier Kraft Board Group of the American Paper Institute, July 15, 1977.
3. Jaeger, T. "A Study of Pressure in the Nip of a Reverse-Roll Adhesive Applicator", M.S. Thesis, May, 1978.
4. Taylor, G. I. "Stability of a Viscous Liquid Contained Between Two Rotating Cylinders," Phil. Trans. A223:289-93(1923).
5. Yih, C. S., Proc. R. Soc. A258:63(1960).

THE INSTITUTE OF PAPER CHEMISTRY


John T. Jurewicz
Research Fellow
Engineering Division

APPROVED BY


Terrence S. Fox
Director
Engineering Division

APPENDIX

STEIN-HALL ADHESIVE

(20% Solids)*

Top Mixer

Primary

Add water	5.520 liters
Add starch	2.4 lb
Increase temperature to 100°F-120°F	
Add sodium hydroxide solution	199 g/1.0 liter
Increase temperature to 180°F and hold 15 minutes	
Add water	

Bottom Mixer

Secondary

Add water	18.0 liters
Add bentonite	123.5 g
Add sodium borate (10 moles)	108.9 g
Add starch	15.15 lb
Add primary slowly - about 30 minutes	
Add water	2.25 liters
Mix 30 minutes	

*The adhesives at different percent solids followed the same formulation with increasing amounts of starch.

STEIN-HALL ADHESIVE

(26.0% Solids)

Primary

Add water	5.246 liters	18.54%
Add starch	2.85 lb	13.68%
Add caustic/water	235.9 g/0.970 mL	2.5%/3.36%
Heat to 135°F-140°F; add caustic solutions; increase temperature to 180°F; hold for 15 minutes		
Add water	2.852 liters	10.08%

Secondary

Add water	17.108 liters	60.46%
Add bentonite	146.2 g	1.55%
Add sodium borate	129.3 g	1.37%
Add starch	17.95 lb	86.32%
Add water after dropping primary	2.139 liters	7.56%

Note: Caustic, bentonite, sodium borate based on weight of dry starch.

IPST HASLTON LIBRARY



5 0602 01057001 0